Effects of Force Fields on Gas Separation Performances of ZIFs

by

Aydın Özcan

A Thesis Submitted to the

Graduate School of Engineering

in Partial Fulfillment of the Requirements for

the Degree of

Master of Science

in

Chemical and Biological Engineering

Koç University

August 2014

Koç University

Graduate School of Sciences and Engineering

This is to certify that I have examined this copy of a master's thesis by

Aydın Özcan

and have found that it is complete and satisfactory in all respects,
and that any and all revisions required by the final
examining committee have been made.

Committee Members:

_____

Seda Keskin Avcı, Ph. D. (Advisor)

_____

Burak Erman, Ph. D.

_____

Metin Türkay, Ph. D.

Date: _____

ABSTRACT

Metal organic frameworks (MOFs) are newly emerging promising candidates for gas separation and gas storage. Zeolitic imidazolate frameworks (ZIFs) are highly robust sub-family of MOFs and they have large surface areas, high porosities and well-defined pore structures.

In the first part of this thesis, Grand Canonical Monte Carlo (GCMC) and Equilibrium molecular dynamics (EMD) simulations are used and a diverse collection of ZIFs are studied to evaluate their performances in adsorption- and membrane-based gas separations. These molecular simulations are performed for both single- component gases (CH_4, CO_2, H_2 and N_2) and binary gas mixtures (CO_2/CH_4, CO_2/N_2, CO_2/H_2 and CH_4/H_2) to predict the intrinsic and mixture selectivities of ZIFs. These two selectivities are compared to discuss the importance of multi-component mixture effects on making predictions about the separation performance of a material. Gas separation performances of ZIFs are compared with other nanoporous materials and results show that several ZIFs can outperform well-known zeolites and metal-organic frameworks in CO_2 separations. Several other properties of ZIFs such as gas permeability, working capacity and sorbent selection parameter are computed to identify the most promising materials in adsorption- and membrane-based separation of CO_2/CH_4, CO_2/N_2, CO_2/H_2 and CH_4/H_2.

In the second part, the effect of different force field parameters on the selectivity estimation is examined. In the literature, a significant number of molecular simulation studies exists for assessing single-component gas adsorption capacities of ZIFs and all these simulations are performed using different force field parameters. Molecular simulations are carried out to predict both adsorption-based and membrane-based separation performances of ZIF-68 and ZIF-69 for CH_4/H_2, CH_4/N_2, CO_2/CH_4, CO_2/N_2 and CO_2/H_2 mixtures using three different force fields. Results show that adsorption selectivity of ZIFs may vary significantly depending on the force field parameters whereas membrane selectivity is much less sensitive to the force field. In addition to adsorption and membrane selectivities, various separation properties of ZIFs are estimated such as working capacity, sorbent selection parameter, regenerability, permeability and compared with the properties of other well-known nanoporous adsorbents and membranes. Results suggest that ZIF-68 and ZIF-69 can outperform traditional zeolites in separation of CH_4/H_2 and CO_2/H_2 mixtures.

ÖZET

Metal organik ağ yapıları yeni ortaya çıkan, gaz depolanması ve gaz ayırım işlemleri için gelecek vaadeden malzemelerdir. Zeolitik imidazolit ağ yapıları da metal organik ağ yapılarının dayanıklılığı oldukça yüksek bir alt grubudur. Zeolitik imidazolit ağ yapıları geniş yüzey alanına, geniş ve sistematik biçimde birbirine bağlanmış gözenek yapılarına sahiptir.

Tezin ilk kısmında, grand kanonik Monte Karlo ve denge halindeki molekül dinamikleri simülasyonları kullanılarak, birçok zeolitik imidazolit ağ yapısının adsorbent ve membran olarak performansları değerlendirildi. Bu moleküler simülasyonlar, zeolitik imidazolit ağların saf gazlar (CH_4, CO_2, H_2 ve N_2) ve karışımlar (CO_2/CH_4, CO_2/N_2, CO_2/H_2 ve CH_4/H_2) için gösterdikleri seçililiğin hesaplanmasında kullanıldı. Ortaya çıkan bu iki ayrı tip seçicilik (yalnız gazlar için ve karışım halindeki gazlar için) karşılaştırılarak, çoklu gaz durumunun seçicilik üzerindeki etkisi tartışıldı. Zeolitik imidazolit ağ yapılarının CO_2 ayırımı için hali hazırda bilinen zeolitlerden daha iyi performansa sahip oldukları gösterildi. Gaz geçirgenliği, gaz taşıma kapasitesi ve sorbent seçilim parametresi gibi başka önemli parametreler de hesaplanarak, değişik gaz karışımları için zeolitik imidazolit ağ yapılarının adsorbent ve membran olarak performansları karşılaştırıldı.

Tezin ikinci kısmında, değişik simülasyon parametreleri seçmenin, seçicilik üzerindeki etkisi araştırıldı. Literatürde, zeolitik imidazolit ağ yapılarının saf gaz adsorpsiyonunu inceleyen çok sayıda makale mevcuttur ve bu makalelerde çoğu kez çok farklı simülasyon parametreleri kullanılmıştır. Literatürde kullanılan simülasyon parametrelerinden üçü alınarak, ZIF-68 ve ZIF-69 malzemelerinde beş farklı gaz karışımı için (CH_4/H_2, CH_4/N_2, CO_2/CH_4, CO_2/N_2 ve CO_2/H_2) tüm seçicilik parametreleri hesaplanmıştır. Sonuçlar adsorpsiyona dayalı seçiciliğin simülasyon parametreleriyle değişkenlik gösterdiğini, hem adsorpsiyon hem de difüzyon hesabını içeren membran seçiciliğinin ise simülasyon parametresi değişikliğinden ciddi biçimde etkilenmediğini göstermiştir. Bu iki seçiciliğin dışında, taşıma kapasitesi, sorbent seçilim parametresi, yenilenebilirlik, geçirgenlik gibi başka özellikler de bilinen zeolitlerle karşılaştırılmıştır. Bu karşılaştırmalarda, ZIF-68 ve ZIF-69, CH_4/H_2 ve CO_2/H_2 karışımları için bilindik zeolitlerden daha iyi performans göstermiştir.

To snow,

ACKNOWLEDGEMENTS

I would like to express my sincere appreciation to my advisor Assoc. Prof. Dr. Seda Keskin for her support, supervision, patience and advices throughout my master process. I obtained Fulbright Scholarship for my PhD applications and it could not be possible without her generous support.

I would like to thank gratefully my thesis committee members Prof. Dr. Burak Erman and Prof. Dr. Metin Türkay for accepting to present in my theses committee. A quote of Prof. Erman in Thermodynamics (ChBi 503) class will be one of the main principles of my future studies: "Axiomatization is a must. Other else is -in a way- stamp-collecting."

I want express my special thanks to officemates. Everything would be much more difficult for me without your support NEMO.

I am also grateful for financial support of TUBITAK BIDEB scholarship for my master studies.

Aydın Özcan

22 July 2014

TABLE OF CONTENT

LIST OF TABLES

LIST OF FIGURES

NOMENCLATURE

μ	Chemical Potential	MAS	Mixture Adsorption Selectivity
Å	Angstrom	MDS	Mixture Diffusion Selectivity
ANA	Analcime	MER	Merlinoite
C	Celcius	MFI	Mordenite Framework Inverted
CBAS	Composition Based Adsorption Selectivity	mmol	Milimole
CH_4	Methane	MMS	Mixture Membrane Selectivity
CHA	Chabazite	MOF	Metal Organic Framework
cm^2	Centimeter square	MOR	Mordenite
CO	Carbon Monoxide	Mpa	Megapascal
Co	Cobalt	N	Number of Molecules
CO_2	Carbon Dioxide	N_2	Nitrogen
COM	Center of Mass	O	Oxygen
D	Diffusivity	P	Permeability
DFT	Density Functional Theory	q	Partial Charge
DMF	N,N-dimethylformamide	Q_{st}	Isosteric Heat of Adsorption
EMD	Equilibrium Molecular Dynamics	r	Distance
FAU	Faujasite	R	Regenerability
FF	Force Field	s	Second
g	Gram	Si	Silicon
GCMC	Grand Canonical Monte Carlo	SOD	Soadlite
GME	Gmelinite	S_{sp}	Sorbent Selection Parameter
H_2	Hydrogen	T	Temperature
IAS	Ideal Adsorption Selectivity	U	Potential
IDS	Ideal Diffusion Selectivity	UFF	Universal Force Field
Im	Imidazolite	V	Volume
IMS	Ideal Membrane Selectivity	XRD	X-Ray Diffraction
J	Flux	ZIF	Zeolite Imidazolite Framework
K	Kelvin	Zn	Zinc
k_B	Boltzman Constant	ΔN	Working Capacity
L	Membrane Thickness	ε	Energy Parameter
LJ	Lennard-Jones	Λ	Thermal Wavelength
LTA	Linda Type A	σ	Size Parameter
M	Metal Atom		

Chapter 1: Introduction

Gas separation is an economically significant process for chemical industry. For example separation of CO_2 from other gases has industrial and environmental effects in a number of large- scale applications. Separation of CO_2 from CH_4 is important in natural gas purification, CO_2/N_2 separation is a key process in carbon capture from flue gas and CO_2/H_2 separation is vital for hydrogen recovery from refineries. Due to global warming and newly upcoming emission regulations, safe and economical separation of CO_2 gained more attention in the last decade. For instance, average surface temperature of the earth is expected to rise around 3 degree due to CO_2 emission in within next century and it is a significant problem for sustainability of life of a lot of entities [1]. Other than such a dramatic effect, CO_2 also has a lot of drawbacks in industrial processes: It is the principal correspondent of pipeline corrosion in natural gas transport and basic impurity in H_2 separation for H_2 recovery from plant and refinery operations.

Gas mixtures are separated by several technologies such as membrane based separation, adsorption and distillation [2, 3]. Some of these separation techniques gain much more importance due to their ability to reduce size of power plants which is called process intensification [4]. In process intensification perspective, membrane-based separations are prominent technologies due to their efficient and operationally clean nature [5].

Synthesis of high surface area and high porosity adsorbents leads to many developments of membrane-based separation technologies. For example, zeolites are one of the most widely used materials in membrane-based separation technology [6]. In the large-scale applications, zeolites, silica gels, activated carbons and metal oxides have a big portion of industrial usage [7]. There is also newly emerging class of membrane materials which are called Metal Organic Frameworks (MOFs). They are brand new materials as candidates for adsorption and membrane-based gas separations due to their high porosity, large surface area, low density,

good chemical and mechanical stability [8-10]. Another important advantage of MOF structures is their chemical and physical tunability during their synthesis over other traditional adsorbent and membrane materials. Zeolite imidazolate frameworks (ZIFs) are a subclass of MOFs that have tetrahedral networks like zeolites with transition metals linked by imidazolate-type linkers [11, 12]. ZIFs have tetrahedral topologies which contain transition metals and imidazolate type of linkers and different combinations of transitions metals with available imidazolate linkers lead a great diversity for ZIFs [13]. Because of the strong interaction between the metal centers and imidazolate linkers, ZIFs have high thermal and moisture stability which make them strong candidates as gas separation devices [14].

Since there are many classes of porous materials which can be used as membrane, it is natural to produce a method and terminology to compare performances of porous materials. Permeability and selectivity are the two fundamental parameters of this terminology to compare the membrane performances [15]. Permeability is the mass transfer rate of gases which float through the membrane. On the other hand, selectivity can be described as the gas separation ability of the membrane. In this respect, mathematical calculation of selectivity is the ratio of permeation rates of gas components. A promising membrane candidate should have high permeability and selectivity [16]. However, permeability and selectivity are trade-off parameters and they are inversely correlated in general [17].

Polymeric membranes are widely used in gas separation processes like air separation and natural gas purification. The permeability-selectivity trade-off is an important drawback for polymeric membranes because more selective polymers are less permeable [17]. To define a limiting selectivity versus permeability performance, Robeson et al. [17] screened over 300 polymeric membrane and determined an upper bound for membrane performance. In 2008, same author made small perturbation on his initial model and updated this upper bound [18].

Zeolite membranes are good alternatives for polymeric membranes since they are able to avoid the trade-off between selectivity and permeability [19]. At that point, ZIFs are very promising candidates for membrane-based gas separation due to their superior properties. Additionally, there is a considerable amount of research on ZIF membranes both experimentally and computationally [20-28].

In this thesis, atomically detailed simulations are performed to assess the membrane performances of ZIFs for CH_4/H_2, CO_2/CH_4, CO_2/N_2, CO_2/H_2, CH_4/N_2 mixtures. Detailed calculations are provided for membrane properties of ZIF-1, ZIF-2, ZIF-3, ZIF-6, ZIF-8, ZIF-

10, ZIF-11, ZIF-12, ZIF-60, ZIF-65, ZIF-67, ZIF-68, ZIF-69, ZIF-78, ZIF-79, ZIF-81, ZIF-90. In Chapter 2, a comprehensive literature survey is provided for adsorption-based and membrane-based separation studies with ZIFs. Chapter 3 describes the basic idea of Grand Canonical Monte Carlo (GCMC) and Equilibrium Molecular Dynamics (EMD) and some terminology which are used in adsorption and diffusion performances of gases in porous materials. In Chapter 4, computational details are discussed. Theoretical calculations used to estimate separation performances of ZIFs for different mixtures are given in Chapter 5. In Chapter 6, the effect of different force field parameters is discussed in detail. Conclusion of this study is presented in Chapter 7.

Chapter 2: Literature Review

2.1. Zeolite Imidazolite Frameworks (ZIFs)

Zeolites are the most important aluminosilicate-based materials which are synthesized to be used in several applications including petroleum refining as catalysis [6]. Zeolites are desirable materials for industrial applications but number of structures is restricted. On the other hand, ZIFs are very tailorable materials and this property leads to synthesis of many different ZIFs in a lot of different way. Additionally, in recent studies, the coincident between the preferred angle of Si-O-Si in zeolites and the bridging angle in the M-Im-M, where M is the metal atom and Im represent the imidazolate, is recognized and this contributes the high robustness of ZIF materials [29]. Furthermore, idea to "programming" the synthesis of ZIFs according to different topologies leads embodiment of new ZIF materials. Using this idea, more than 90 new structures named as ZIFs were synthesized in recent years [29].

ZIFs are one of the most widely studied subfamilies of Metal Organic Frameworks (MOFs) which are constructed from tetrahedral metal ions such as Zn and Co bridged by imidazolate. As described earlier, the similarity between angles of the Si-O-Si and M-Im-M has conducted of the synthesis of extensive amount of ZIF structures with zeolite-type tetrahedral topologies [29]. Originated from the angle similarity, ZIFs exhibit extensively good chemical and thermal stability. In addition to the stability, ZIFs possess important properties including permanent and high porosity, large surface area and tailorable pore sizes. All these properties have led ZIFs to be ideal candidates for gas storage and separation processes.

ZIFs are generally synthesized using a generic synthesis procedure developed by Yaghi's research group [30]. During synthesis procedure, the desired hydrated transition metal salt is

combined with the ImH unit in an amide solvent such as DMF (N,N-dimethylformamide). Then the solution is heated to temperatures changing between 85 and 150 ˚C. The linking of ImH is deprotonated by amines and the thermal degradation of the solvent is achieved under these conditions. The critically important parameters to achieve monocrystalline ZIFs are the molar ratio and the concentration of metal ion and the reaction temperature. A variety of ZIFs synthesized possess the zeolite topologies such as Analcime (ANA), Chabazite (CHA), Faujasite (FAU), Gmelinite (GME), Linda Type A (LTA), Merlinoite (MER), (Mordenite Framework Inverted (MFI), mordenite (MOR) and Sodalite (SOD) [30, 31].

2.2. Literature Review on ZIFs

ZIFs have been synthesized with a diverse range of pore dimensions, topologies, chemical functionalities and they exhibit high thermal and moisture stability which are desired properties in adsorption-based and membrane-based gas separations. Since early 2000s, Yaghi's research group synthesized several ZIF structures and performed detailed experiments of those materials with the purpose of gas storage and separation. For example, Park and coworkers [29] synthesized twelve ZIFs, termed ZIF-1 to ZIF-12, and studied gas adsorption in these frameworks. They concluded that several ZIFs demonstrate exceptionally high thermal stability up to 550 ˚C and remarkable chemical resistance to boiling alkaline water and organic solvents. Similarly, Banerjee et al. [30] synthesized twenty five ZIFs also exhibiting high thermal stability and permanent porosity with surface areas up to 3900 m^2/g. They reported that ZIF-68, ZIF-69 and ZIF-70 which exhibit chemical stability in refluxing organic and aqueous media possess unusual selectivity for CO_2 over CO. Additionally, Morris et al. [32] synthesized ZIFs, ZIF-90, ZIF-91 and ZIF-92, and concluded that useful organic transformations can be performed on ZIFs without altering their structural integrity. The studies conducted by Yaghi's research group have specified the direction of studies related with ZIFs. Various research groups also examined these materials as both adsorbent and membrane candidates. It has been reported that gas adsorption and transport properties of ZIFs should be investigated carefully since the structural properties of these materials are highly promising [21, 33].

In several computational and experimental studies, ZIFs are identified as promising adsorbents. ZIFs show high adsorption selectivity towards CO_2 over other gases such as CH_4, CO, N_2. For example, Banerjee et al. [30, 34] synthesized ZIFs having the same topology,

ZIF-68, ZIF-69, ZIF-70, ZIF-78, ZIF-79, ZIF-80, ZIF-81 and ZIF-82, and examined CO_2 capture capabilities of these materials. Additionally, Wang et al. [12] synthesized ZIF-95 and ZIF-100 which have large cavities and highly constricted pores and reported that these ZIFs exhibit higher affinity for CO_2 over CH_4, CO and N_2 at room temperature. They had pointed out that high selectivity for CO_2 is affected by the strong quadrupolar interactions of CO_2 with the N atoms present on the pore surface. Park et al. [29] examined the performance of ZIF-8 and ZIF-11 as adsorbents for H_2 separation at 77 K. At low pressures, H_2 uptake in ZIF-11 is high with respect to other ZIFs considered since ZIF-11 structure has to the benzene rings that create favorable H_2 adsorption sites at low pressure range. As pressure increases, the physical properties of the ZIF structures such as surface area and pore volume become dominant and affect H_2 adsorption. Consequently, although ZIF-8 adsorbs lower amount of H_2 at low pressure range, it exhibits high H_2 adsorption at higher pressures due to its larger pores.

ZIFs such as ZIF-7, ZIF-8, ZIF-22, ZIF-69, ZIF-78 and ZIF-90 are also studied as membrane candidates to separate several gas mixtures. Li et al. [35] synthesized ZIF-7 membrane and investigated gas separation performances of ZIF-7 membrane at 200 °C and 1 bar. They reported the permeances of pure CH_4, CO_2, H_2 and N_2 and the permeances of components in equimolar mixtures of H_2/CH_4, H_2/CO_2 and H_2/N_2. They investigated ZIF-7 membrane specifically since its pore size (3.0 Å) seems ideal to separate H_2 (2.9 Å) from larger gas molecules. Consequently, ZIF-7 showed molecular-sieving effect due to its pore size which is slightly larger than the kinetic diameter of H_2 and smaller than the kinetic diameter of other gases. ZIF-7 membrane was also reported to exhibit good thermal and hydrothermal stabilities. Bux et al. [24] fabricated ZIF-8 membranes and measured the permeances of CH_4, CO_2, N_2 and O_2, as single components and the permeances of H_2 and CH_4 in equimolar mixture at room temperature. Their results indicated that permeation of H_2 molecules slow down in the presence of slow CH_4 molecules. Huang et al. [22] reported the permeances of pure CO_2, H_2, N_2 and O_2 and the selectivities of H_2 over CO_2, N_2 and O_2 (in equimolar mixtures) for ZIF-22 membrane at 323 K and atmospheric pressure. Separation factors were measured as 7.2, 6.4, 6.4 and 5.2 for H_2/CO_2, H_2/O_2, H_2/N_2 and H_2/CH_4, respectively. Dong et al. [36] fabricated ZIF-78 membrane and measured the permeances of H_2, CO_2, N_2 and CH_4. They concluded that ZIF-78 is H_2 selective membrane over CH_4, CO_2

or N_2. Huang et al. [23] fabricated ZIF-90 membranes and studied H_2/CO_2 separation. They reported that ZIF-90 is a H_2 selective membrane.

Molecular simulations have been widely used to predict gas adsorption and transport properties of ZIFs. For example, Guo et al. [38] investigated CH4/H2 separation in ZIF-3, ZIF-8, ZIF-10, ZIF-60 and ZIF-67 as well as IRMOF-1 (also named as MOF-5) performing Grand Canonical Monte Carlo simulations (GCMC). IRMOF-1 exhibits the highest H_2 and CH_4 uptake due to its large pore volume compared to ZIFs. However, IRMOF-1 shows selectivity of CH_4 over H_2 less compared to ZIFs. The reason is the fact that narrow pores of ZIFs with respect to IRMOF-1's allow ZIFs to have higher selectivity of CH_4. Han et al. [37] studied H_2 uptake in several ZIFs including ZIF-2, ZIF-3, ZIF-8, ZIF-10, ZIF-11, ZIF-68, ZIF-69, ZIF-70, ZIF-78 and ZIF-79 at 77 and 298 K up to 100 bar. They observed that H_2 uptake is correlated with the type of functional groups at low pressures (between 2 and 10 bar), since adsorption is affected by polarity of the functional group as well as surface area and pore topology at this pressure region. At higher pressures, H_2 uptake of ZIFs is found to be dependent on surface area and pore volume. Similarly, Chen et al. [38] studied H_2 adsorption in ZIF-68, ZIF-69, ZIF-78, ZIF-79 and ZIF-81 at 77 K up to 80 bar. They concluded that effective porosity affects hydrogen uptake in ZIFs at high pressures. Liu and Smit [39] studied adsorption of CO_2/N_2, CO_2/CH_4 and CH_4/N_2 mixtures in ZIF-68 and ZIF-69. Their results indicated that ZIF-69 is more beneficial to capture CO_2 from these mixtures. Liu et al. [40] reported self-diffusion coefficient of CO_2 in ZIF-68 and ZIF-69. They concluded that the small pores formed by the nIM linkers in ZIF-68 and ZIF-69 are the preferential adsorption sites for CO_2 molecules and the corners formed by the phenyl rings in the large pores are less preferential adsorption sites. Rankin and co-workers [41] studied adsorption and diffusion behaviors of CO_2, CH_4, N_2 and H_2 in ZIF-68 and ZIF-70 using GCMC and EMD simulations. In this work, they investigated the charge contribution to the uptake predictions in these ZIFs and concluded that agreement between the experiments and simulations is very good when quadrupole interactions included. Krishna and van Baten [42] computed diffusivities of CO_2/H_2 and CH_4/H_2 mixtures in ZIF-8 and CO_2/CH_4 mixtures in ZIF-68 whereas Keskin [43] studied adsorption and diffusion of CH_4/H_2, CO_2/CH_4, and CO_2/H_2 mixtures in ZIF-3 and ZIF-10. Similarly, Liu et al. [44] investigated adsorption of CO_2/CH_4 and CH_4/H_2 mixtures in ZIF-68 and ZIF-70 and Wu et al. [45] screened several

ZIFs for adsorption-based separation of CH_4/H_2 mixtures. Huang and co-workers [46] investigated adsorption of CO_2, CO, CH_4 and N_2 in ZIF-8 and predicted the selectivities for CH4 over CO, N_2 and CO_2 over CH_4, CO, N_2 using Henry's law constants of the single component adsorption isotherms at 273, 298, 323 and 348 K. They reported that the selectivities are strongly correlated with the differences of isosteric heat of adsorption (Q_{st}) between the two components. As the difference of Q_{st} between the two components increases, the selectivity also increases. As stated earlier, most studies have focused on only one or a few ZIFs at a time and these studies have examined the potential of ZIFs generally for adsorption-based separation of CH_4/H_2 or CO_2/CH_4 [41, 46]. Therefore, a diverse collection of sixteen ZIFs are investigated and their performances in adsorption-based and membrane-based CO_2/CH_4, CO_2/N_2, CO_2/H_2 and CH_4/H_2 separations are explored in the first part of this study.

The accuracy of a molecular simulation strongly depends on the type of force field used in the simulation. Different research groups used different force fields for gas adsorption simulations of ZIFs and compared their simulated results with the available experimental data either to validate the accuracy of parameters or to refine their parameters in order to match the simulation results with the experiments. For example, Liu and coworkers [40] calculated CO_2 adsorption in ZIF-68 and ZIF-69 using grand canonical Monte Carlo (GCMC) simulations with UFF (Universal Force Field); Liu and Smit [39] computed adsorption of CO_2, CH_4 and N_2 in ZIF-68 and ZIF-69 using GCMC with UFF and a new set of force field (FF) that they defined; Babarao et al. [47] studied adsorption of CO_2, CH_4, N_2 and H_2 in ZIF-68 and ZIF-69 using GCMC simulations based on two generic FFs, UFF and DREIDING; Sirjoosingh et al.[48] simulated CO_2 and CO adsorption in ZIF-68 and ZIF-69 using UFF; Hou and Li [49] studied CO_2 adsorption in ZIF-68 and ZIF-69 using UFF; Prakash et al. [50] also simulated H_2, N_2, CH_4 adsorption in ZIF-95 and ZIF-100 using self-calculated Morse potential parameters; Li et al. [51] evaluated N_2, CH_4, CO_2 selectivity of ZIF-78 and ZIF-79 using UFF, DREIDING and refined UFF parameters.[39]

The number of studies on gas diffusion simulations of ZIFs is very limited compared to gas adsorption simulations. Using UFF, Rankin et al. [52] reported diffusion of H_2, CH_4 and CO_2 in ZIF-68 and ZIF-70; Sirjoosingh and co-workers [48] examined diffusion of CO_2 and CO in ZIF-68 and ZIF-69; Liu et al. [40] studied CO_2 diffusion in ZIF-68 and ZIF-69;

Babarao et al. [47] examined diffusion of CO_2 in ZIF-68. Atci and Keskin [53] reported the first data for mixture diffusion in ZIFs by computing self-diffusivities of CH_4/H_2, CO_2/CH_4, CO_2/H_2 mixtures in 15 different ZIFs using UFF and DREIDING. A significant number of molecular simulation studies exist in the literature for assessing single-component gas adsorption capacities of ZIFs and all these simulations are performed using different force field parameters. In the second part of this work, molecular simulations are employed to predict both adsorption-based and membrane-based separation performances of ZIF-68 and ZIF-69 for CH_4/H_2, CH_4/N_2, CO_2/CH_4, CO_2/N_2 and CO_2/H_2 mixtures using three different force fields. The effect of force field on evaluating separation performances of these ZIFs is analyzed in detail.

2.3. Important Gas Separations

ZIFs have attracted the interest of both academia and industry in several applications including gas storage, gas separation, catalysis, drug storage and sensing [5, 27]. Since gas storage and separation applications have crucial role in industry and energy-related researches, they are the most mature application areas of ZIFs.

Pure gases such as CH_4, CO_2, H_2 and N_2 have very important usage in various industrial applications. For example, the need for H_2 has increased in chemical manufacturing and petroleum refining applications [6, 8]. Since the oxidation product of H_2 is water, using H_2 is advantageous especially in energy applications. Similar with H_2, CH_4 can also be used in energy applications. Consequently, materials exhibiting high storage capacity for H_2 and CH_4 have crucial role in energy-related applications. Since clean energy research has gained importance because of the exhaustion of fossil oil deposits and the growing threat of global warming, several research groups search for clean energy carriers such as H_2 and CH_4 as well as they attempt to find a way to reduce CO_2 emissions. Apart from H_2 and CH_4 related studies, CO_2 capture has gained interest due to several other reasons including large-scale industrial applications [42]. Such applications indicate that the storage of single component gases is very important and can be used for several purposes. In this thesis, adsorption-based separation performances of ZIFs for CH_4, CO_2, H_2 and N_2 have been studied to identify good adsorbent candidates which can be used in industrial applications.

Separation of gas mixtures has significant application area of ZIFs. In this work, ZIFs have been studied to separate CH_4/H_2, CH_4/N_2, CO_2/CH_4, CO_2/N_2 and CO_2/H_2 mixtures since

they are industrially and economically important. For example, CH_4/H_2 and CH_4/N_2 separation are crucial for purification of synthesis gas which is obtained from steam reforming of natural gas. Since pure H_2 and N_2 have several industrial applications including chemical processes, medical and pharmaceutical applications, these separations are good examples of large-scale industrial applications. To separate CO_2 from H_2 is relevant for H_2 recovery from plants and refineries. Separation of CO_2/CH_4 separation is vital for natural gas purification and separation of CO_2 from N_2 is important in carbon capture from flue gas.

Adsorption-based and membrane-based separation processes are advantageous ways for separation applications. For adsorption-based separation applications, adsorbents should adsorb the desired gas molecules with the desired amount whereas in the membrane-based processes, material's capabilities for adsorption and diffusion of the desired component are crucial. Therefore, adsorption and diffusion behaviors CH_4/H_2, CH_4/N_2, CO_2/CH_4, CO_2/N_2 and CO_2/H_2 mixtures in ZIFs are investigated in this work.

Chapter 3: Theoretical Background

In this chapter, Grand Canonical Monte Carlo (GCMC) and Equilibrium Molecular Dynamics (EMD) simulation methods are described and definition of permeability is introduced.

3.1. Modeling Adsorption Isotherms with Atomistic Models

In this study, adsorption of gases in Zeolite Imidazolate Frameworks (ZIFs) is calculated by GCMC simulations. In this part, details of GCMC method are briefly given. GCMC is an attractive methodology for this study because it could generically replicate experimental measurements of gas adsorption. In the formulation of grand canonical ensemble, the temperature, volume, and chemical potential are fixed. In GCMC simulations, particles' transfer between the adsorbent phase and gas phase due to their chemical potential difference. When system reaches to equilibrium, the temperature and chemical potential of the insider gas and outsider gas must be equal [54]. After equilibrium is established, total number of adsorbed gas molecules fluctuates around its equilibrium value. GCMC simulation results can be directly compared with experimental adsorption measurements [33, 55, 56].

To illustrate the details of the GCMC method, the grand partition function is shown in Equation (3.1) [57].

$$Z_g(\mu, V, T) = \sum_{N=0}^{\infty} \frac{e^{\beta\mu N} V^N}{\Lambda^{3N} N!} \int dr^N e^{-\beta U(r^N)} \tag{3.1}$$

In Equation (3.1), N is the number of particles in simulated system, μ is the chemical potential of adsorbing species, Λ is the thermal wavelength (correspondence of momentum of adsorbing gas Hamiltonian), $\beta = (k_B T)^{-1}$, k_B is Boltzman constant and T is the temperature. $U(r^N)$ is the interaction potential between N particles where r^N is the position vector of the N adsorbed molecules and V is volume of the system. As a generic procedure in statistical

mechanics, the mean value of desired variable can be generated by taking derivative of generated partition function as shown in Equation (3.2).

$$\langle N\rangle = k_B T \frac{\partial \ln(Z_g)}{\partial \mu} \tag{3.2}$$

However, there is a serious problem to calculate such a variable due to complexity of $\int r^N e^{-\beta U(r^N)}$ (a multidimensional integral) which is in the partition function. To overcome this computational complexity, Metropolis sampling method [54] proposes a numerical framework. The method proposes random configurations based on the probability stated as Equation (3.3).

$$\mathrm{Prob}(N, r^N) = \frac{\dfrac{e^{\beta\mu N} V^N \int r^N e^{-\beta U(r^N)}}{\Lambda^{3N} N!}}{Z_g} \tag{3.3}$$

In a Markovian scheme, Metropolis method generates a random chain of events (simply called insertion, deletion and displacement) which determine whether system seals from an old state (o) to new state (n). For these moves, the acceptance probability of sealing from a state to another state is obtained from detailed balance principle based on the difference between total potential energy.

Insertion
$$(N_{acc} \to N+1) = \min\left(1, \frac{V e^{\beta(\mu-\Delta U)}}{\Lambda^3 (N+1)}\right) \tag{3.4}$$

Deletion
$$(N_{acc} \to N-1) = \min\left(1, \frac{\Lambda^3 N e^{-\beta(\mu-\Delta U)}}{V}\right) \tag{3.5}$$

Displacement
$$(s_{acc} \to s') = \min\left(1, e^{-\beta \Delta U}\right) \tag{3.6}$$

The energy difference term corresponds to difference between trial configuration and initial configuration. To decide to generate new move, acceptance probability is compared with randomly created number within the interval of 0 and 1 [54].

3.2. Modeling Diffusion with Atomistic Simulations

3.2.1. Transfer of Matter by Diffusion

The description of diffusion based on Adolf Fick's work can be simply constituted as shown in Equation (3.7) where D represents diffusivity.

$$J = -D\nabla c \tag{3.7}$$

This equation relates the concentration gradient (∇c) to flux (J) by defining diffusivity. Equation of continuity implies the following equation by using Fick's diffusivity equation:

$$\frac{dc}{dt} = \nabla \times (D\nabla c) \underset{D\,\text{constant}}{\Rightarrow} \frac{dc}{dt} = D(\nabla^2 c) \tag{3.8}$$

To assign D as a constant is a simple assumption. Fick's law carries out the implication that concentration gradient is the driving force of diffusion. On the other hand, diffusion is simple manifestation of tendency to reach the equilibrium configuration, so it is reasonable that the true driving force must be chemical potential gradient. This point is clarified by Einstein when he was working on explaining the random walk phenomena. According to this assumption, gradient of chemical potential and frictional forces should be in equilibrium in steady state energy balance for a volume element as represented in Equation (3.9).

$$\zeta v_A = -\frac{d\mu_A}{dz} \tag{3.9}$$

In Equation (3.9), v_A is flow velocity and ζ stands for the friction coefficient of component A. Although the model can also be easily generalized to more dimensions, gradient is taken along one axis (z) to simplify the model in Equation (3.9). The flux (J_A) is equal to $v_A c_A$ where c_A is the concentration of component A. Additionally, the Equation (3.10), derived for equation state of an ideal gas, can be used to relate chemical potential to concentration [58].

$$\mu_A = \mu_A^0 + RT\ln(p_A) \tag{3.10}$$

By using Equations (3.9) and (3.10), a flux equation can be constructed as in Equation (3.11).

$$J_A = v_A c_A = -\frac{RTc_A}{\zeta}\frac{d\ln(p_A)}{dz} \tag{3.11}$$

To resemble this equation to Fick's diffusion equation, the chain rule property of derivatives can be used.

$$J_A = -\frac{RT}{\zeta}\frac{d\ln(p_A)}{d\ln(c_A)}\frac{dc_A}{dz} \tag{3.12}$$

Since Equation (3.12) is in the form of Fick's first law, Equation (3.1), the transport diffusivity can be calculated using Equation (3.13).

$$D_A = \frac{RT}{\zeta}\frac{d\ln(p_A)}{d\ln(c_A)} = D_0\frac{d\ln(p_A)}{d\ln(c_A)} \tag{3.13}$$

In the last part of this equation D_0 term is appeared and it is named as corrected diffusivity (sometimes also referred as Maxwell-Stefan Diffusivity). It is simply the relation between thermal smearing (thermal noise on the particle) and friction coefficient which comes from the physics of media that particles seal in it.

Transport diffusivity and corrected diffusivity are not the only parameters which are defined for describing macroscopic diffusion. There is one more diffusion coefficient called self-diffusion coefficient which based on studies of Einstein to explain Brownian. Einstein had started form Equation (3.2) and had estimated that concentration has a Gaussian distribution as a solution Equation (3.2). Then, he had proposed that mean-square displacement can be calculated by using this Gaussian distribution function. The result is given in Equation (3.14).

$$\langle r^2(t)\rangle = \int r^2 \frac{e^{-\frac{r^2}{4Dt}}}{(4\pi\ Dt)^{3/2}} dr = 6D_s t \tag{3.14}$$

Equation (3.14) is generally known as Einstein's relation and gives a direct relation between diffusivity and time dependence of mean square displacement which known to be most easily observable quantity of Brownian Motion [59].

It is possible to relate transport diffusivity, corrected diffusivity and self-diffusivity with Onsager's phenomenological constant [60].

3.2.2. Obtaining Diffusion Coefficients from EMD Simulations

Before starting the details of diffusion coefficients calculations, Equilibrium Molecular dynamics (EMD) simulation methodology will be explained briefly in this section. EMD simulates the time evolution of molecules by way of solving Newton's equation of motion [54]. The result of this evolution leads to structural and thermodynamics properties of material. The Newton's second law is given in Equation (3.15) where F_i is the force exerting on the particle i and m_i and r_i are mass and position of the particle.

$$F_i = m_i \times \frac{d^2 r_i}{dt^2} \tag{3.15}$$

Trajectory for every particle can be obtained by solution of this equation. There are many numerical methods available for integrating the equation of motion. The most widely used algorithm to solve these equations is Velocity-Verlet algorithm and it is based on second order Taylor expansion. The position and velocity of a particle at time t+Δt can be calculated if the position and the velocity of the particle at time t are known.

$$r(t+\Delta t) = r(t) + \Delta t \times v(t) + \frac{(\Delta t)^2}{2} \times \frac{F(r(t))}{m} \tag{3.16}$$

$$v(t+\Delta t) = v(t) + \Delta t \times \frac{\left(F(r(t+\Delta t)) + F(r(t))\right)}{2m} \tag{3.17}$$

Firstly, r(t+Δt) is solved using Equation (3.16) and then F(r(t+Δt)) term is updated in Equation (3.17) since force can be calculated using the relation of $F(r(t))=-\nabla U(r(t))$. Then, by using F(r(t)) and F(r(t+Δt)), v(t+Δt) will be updated and chain will iterate in this direction.

Macroscopic diffusion can be described as self-diffusion (D_s), corrected diffusion (D_0) and transport diffusion (D_t) discussed earlier. Self-diffusivity is mainly individual mobility of molecules and can be interpreted using Equation (3.18).

$$D_s = \lim_{t\to\infty} \frac{1}{6t} \langle \frac{1}{N} \sum_{k=1}^{N} \left[r_k(t) - r_k(0) \right]^2 \rangle \tag{3.18}$$

In Equation (3.18), N is the number of the molecules where c and $r_k(t)$ stand for the concentration and the position of the k^{th} particle at time t, respectively.

Another definition of the diffusion is transport diffusivity (D_t) which is directly related with diffusion through the membrane. The relation between transport diffusivity (D_t) and corrected diffusivity (D_0) can shown using Equation (3.19).

$$D_t(c) = D_0(c) \frac{d\ln(f)}{d\ln(c)} \tag{3.19}$$

In Equation (3.19), f is the fugacity and it can be replaced with pressure in ideal gas equation of state. Using Equation (3.19), transport diffusivity can be calculated via corrected diffusivity which can be computed using Equation (3.20).

$$D_0 = \lim_{t\to\infty} \frac{1}{6N} \langle \left(\sum_{k=1}^{N} \left(r_k(t) - r_k(0) \right) \right)^2 \rangle \tag{3.20}$$

Equation (3.20) generalizes the idea that diffusion can be calculated by the positions of N distinct molecule in the adsorbed phase and to minimize statistical errors these calculations should be repeated and saved through as different trajectories.

In general diffusion coefficients are concentration dependent and unequal to each other. However one important equation between them holds in infinite dilution limit. For very dilute cases, all three diffusion coefficients are equal to each other.

$$\lim_{c\to 0} D_t(c) = \lim_{c\to 0} D_0(c) = \lim_{c\to 0} D_s(c) \tag{3.21}$$

3.2.3. Modeling Mass Transfer through Membrane

Membrane-based gas separation performance of a material depends on both diffusion and adsorption of gases in materials. For single gas permeability, calculation of net flux of gas through the membrane is required. To calculate flux, Fickian diffusivity which given in Equation (3.8) is required. However, to calculate D_t, D_0 must be calculated from EMD simulations. Then the product of corrected diffusivity and thermodynamic correction factor which is calculated from GCMC simulations gives transport diffusivity. Additional the concentration gradient could be calculated using Equation (3.22).

$$\nabla c = \frac{c_2 - c_1}{L} \tag{3.22}$$

In Equation (3.22), c_2 is permeate side concentration, c_1 is the feed side concentration and L is the membrane thickness. After calculating the flux, the single gas permeability is calculated as shown in Equation (3.23).

$$P = \frac{J}{(\Delta p)/L} \tag{3.23}$$

For mixtures, permeability calculations are in a different scheme. Pioneering work of Krishna generated a general framework to calculate membrane permeability for mixture gases as explained in his study [42].

$$P = \frac{\varphi \times D_{i,self} \times c_i}{f_i} \tag{3.24}$$

In Equation (3.24), φ, D_{iself}, c_i and f_i represent fractional pore volume, self-diffusivity, concentration, and fugacity of the i^{th} component, respectively.

Chapter 4: Computational Details

In this chapter, models used to describe gas molecules and ZIFs (Zeolite Imidazolite Frameworks) are briefly discussed as well as other computational details. Additionally, the parameters which are used to evaluate adsorbent and membrane candidates are introduced.

4.1. Models for ZIFs and Gas Molecules

17 different materials, ZIF-1, ZIF-2, ZIF-3, ZIF-6, ZIF-8, ZIF-10, ZIF-11, ZIF-12, ZIF-60, ZIF-65, ZIF-67, ZIF-68, ZIF-69, ZIF-78, ZIF-79, ZIF-81 and ZIF-90 are studied throughout this thesis. The atomic positions of ZIFs are taken from experimental X-ray diffraction (XRD) studies and solvent-free, rigid structures are used in all molecular simulations [29, 30, 32, 34]. Rigid framework assumption gives reasonable agreement with experimental data for a lot of structures and it was validated by previous effort of Kiselev and co-workers [61] for nonpolar molecules in zeolites. When framework is assumed to be rigid, there is no need to model the zeolite-zeolite interactions. In a more realistic perspective, frameworks should be considered as flexible by considering vibrational modes for framework-framework interactions. Although a considerable amount of research continues on flexible structures [62-65], there is no commonly accepted flexible force field parameters in the literature. Even though some of them seem promising [64], the studies are quite premature in this field. Additionally, simulations with flexible framework assumption bring significant computational cost. For example, two orders of magnitude CPU (Central Processing Unit) time is needed to study very low concentration adsorption in flexible structures [66].

4.2. Models for Intermolecular Interactions

Adsorbate-adsorbate interactions and adsorbate-adsorbent interactions should be well defined for a reliable simulation in a gas-porous material system. Lennard-Jones (LJ) and Coulomb potentials are the most suitable candidates to describe such interactions. Although other forms also exist, 12-6 type LJ potentials are used in this thesis. LJ potential defines non-bonded pair-wise repulsive and attractive interactions between gas-gas and gas-adsorbent interactions. The equation for LJ potential can be deduced as stated in Equation (4.1).

$$U_{LJ}(r_{ij}) = 4\varepsilon_{ij}\left[\left(\frac{\sigma_{ij}}{r_{ij}}\right)^{12} - \left(\frac{\sigma_{ij}}{r_{ij}}\right)^{6}\right] \tag{4.1}$$

In this equation, ε_{ij} is the energy parameter between i^{th} and j^{th} atoms whereas σ_{ij} is the distance LJ parameter and LJ potential ($U_{LJ}(r_{ij})$) can be calculated by using this parameters. The LJ potential is the function of distance (r_{ij}) between two interacting atoms. The r^{-6} part of this equation describes the attractive interaction between two atoms. This relation between pair-wise attractive interaction can be demonstrated by exploiting time-independent perturbation theory in quantum mechanics [67]. The r^{-12} part is simple fitting to describe between repulsion effects between two atoms when they are close to each other. Inserting r^{-12} for repulsion in LJ potential gives reasonable results for mimicking the physisorption phenomena. Researchers could insert other repulsion term such as r^{-10} for water models or could take Morse potential as repulsion term for mimicking chemisorptions [68].

It can be seen that, to make calculation with LJ potentials in Equation (4.1), a set of energy and displacement parameters needed. In most simulation studies the adsorbent-adsorbate interaction parameters are obtained from fitting to experimental data. The fitting procedure brings uncertainties in the model and getting a unique set of parameters is not commonly possible. To exemplify the possible uncertainties, parameters can be obtained from fitting experimental result of diffusion coefficients, heat of adsorptions or Henry gas constant in different studies and these different choices could lead to attain different set of parameters. The difficulties to obtain a reliable data set have been emphasized by Dubbeldam et al. [69].

Defining reliable parameter sets is crucial for simulation studies. On the other hand, there is not commonly available accurate experimental data as Pascual et al. [70] pointed out previously. Therefore, Lorentz-Berthelot mixing rules sketch a scheme for defining interaction parameters between gas atoms and frameworks atoms. According to this mixing

rule mix-displacement (mix-energy parameters) parameters are determined by arithmetic mean of self-displacement parameters (geometric mean of the self-energy parameters).

$$\sigma_{ij} = \frac{\sigma_i + \sigma_j}{2} \tag{4.2}$$

$$\varepsilon_{ij} = \sqrt{\varepsilon_i \varepsilon_j} \tag{4.3}$$

Coulomb potential is another important potential term between the atoms in the simulation box. Coulomb potential describes only interactions between charged atoms and the basic difference from LJ potentials. The Coulomb potential between two charged particles can be calculated with Equation (4.4).

$$U_C(r_{ij}) = \frac{1}{4\pi\varepsilon}\frac{q_i q_j}{r_{ij}^2} \tag{4.4}$$

Coulomb potential is a function of inter-atomic distance (r_{ij}). q_i and q_j are the electron charge of i^{th} and j^{th} atoms and ε represents electromagnetic permittivity of vacuum. The total potential on a selected charged atom is the sum of LJ potential and Coulomb potential on the atom.

The basic potential to define the force on an atom requires the specified set of parameters. Energy and distance parameters are needed for LJ potentials, parameterized charges are needed for Coulomb potentials. Three main force field parameters which are, commonly used in ZIFs literature are developed to calculate the LJ potentials between atoms. These three force fields are Universal Force Field (UFF) [71], DREIDING [72] and considerably new parameter set which is generated by Liu et al. [39]. This new parameter set will be referred as Liu FF in upcoming discussions. UFF is used in the study represented in Chapter 5 and three force fields (UFF, DREIDING, Liu FF) are used in the study of Chapter 6. Additionally, different gas models and charge assigning methods are employed in Chapter 5 and Chapter 6 and these differences can be listed as following.

In Chapter 5, 16 different ZIFs are studied and only UFF parameters are used in the simulations. Atci et al. [73] showed that the results of molecular simulations employing UFF agree well with the experimental measurements of gas permeances and permeabilities through ZIF membranes. Spherical LJ 12-6 potentials are used to model H_2 and CH_4 molecules [74, 75]. The CO_2 molecule is modeled as a rigid linear molecule which is an all-atom LJ potential

with atomic charges to approximate CO_2's quadrupole moment [76]. The N_2 molecule is represented as a three site model with two sites located at two N atoms and the third one located at its center of mass (COM) with partial point charges [77]. Partial point charges are defined for ZIF atoms for the simulations of CO_2 and N_2 molecules. Partial point charges for all ZIFs except ZIF-90 are assigned using the connectivity-based atom contribution (CBAC) [78]. This method assumes that the partial charge of an atom in a framework is determined by its bonding connectivity and the atoms with the same connectivity have identical charges. The atomic partial charges of ZIF-90 are defined using REPEAT charges of Watanabe et al. [79].

Table 4.1 Potential parameters used for gas molecules in molecular simulations discussed in Chapter 5.

Molecule	**Atom**	**σ (Å)**	**ε/k_B (K)**	**q(e)**
H_2	H_2	2.96	34.20	-
CH_4	CH_4	3.73	148.20	-
CO_2	C	2.80	27.00	0.70
	O	3.05	79.00	-0.35
N_2	N	3.31	36.40	-0.40
	COM	0.00	0.00	0.80

Table 4.2 Potential parameters used for gas molecules in molecular simulations discussed in Chapter 6.

Molecule	**Atom**	**σ (Å)**	**ε/k_B (K)**	**q(e)**
H_2	H_2	2.96	34.20	-
CH_4	CH_4	3.72	158.50	-
CO_2	C	2.78	29.66	0.57
	O	3.01	82.96	-0.28
N_2	N	3.31	36.00	-0.48
	COM	0.00	0.00	0.96

In Chapter 6, performances of ZIF-68 and ZIF-69 are evaluated by using three different force field parameter sets and the framework charges are taken from the Density Functional Theory (DFT) calculations of ZIF-68 and ZIF-69 [39, 40]. H_2 model remains same as given

above and CH_4 is modeled as united atoms, single-centered LJ molecules and their potential parameters are taken from Dubbeldam et al. [69]. The CO_2 molecule is modeled rigid and linear. Its quadrupole charges and potential parameters are taken from the Hirotani et al. [80]. The N_2 molecule is modeled as a diatomic molecule and its quadrupole charge and potential parameters are taken from TraPPE [76].

4.3. Performance Evaluation of ZIFs

A lot of different parameters have defined to evaluate the performance of ZIFs as an adsorbent and membrane for separation of gas mixtures. Calculation of these evaluation parameters requires mixture GCMC and mixture EMD simulations which are computationally demanding. Due the computational complexity of mixture simulations, there are also alternative formulations for evaluation parameters which are needed less computational time. The alternative approach is to perform single gas simulations and making calculations according to these simulations. The details of these approaches will be elaborated in following paragraphs.

As it is briefly introduced, adsorption, diffusion and membrane selectivities of ZIFs for mixture gas separations can be calculated by using both single-component and mixture simulation data. Results obtained from molecular simulations of single-component gases can be used to predict intrinsic selectivity of ZIFs, such as ideal adsorption selectivity, composition-based adsorption selectivity, ideal diffusion selectivity and ideal membrane selectivity. Ideal adsorption selectivity (IAS) of component i from component j is calculated as a ratio of single-component adsorbed amounts of gases which generated by single GCMC simulations.

$$IAS_{(i/j)} = \frac{c_i^{pure}}{c_j^{pure}} \tag{4.5}$$

Composition-based adsorption selectivity (CBAS) is calculated as the ratio of single-component adsorbed amounts of gases at the specified partial pressures of each component corresponding to mixture compositions.

$$CBAS_{(i/j)} = \frac{c_i^{pure} / c_j^{pure}}{y_i / y_j} \tag{4.6}$$

For example, if the adsorption pressure is set to 10 bar and composition of the mixture is 50/50, single component adsorption amount of each gas component is calculated at 5 bar. In the above expressions, c_i^{pure} is the adsorbed loading of single component i calculated from GCMC and y_i is the molar fraction of the component i in the bulk gas phase.

Results obtained from molecular simulations of binary gas mixtures can be used to predict mixture selectivity of ZIFs such as mixture adsorption selectivity, mixture diffusion selectivity and mixture membrane selectivity even though performing such simulation is considerably computational time demanding. Mixture adsorption selectivity (MAS) is calculated as the ratio of adsorbed amounts of components in their binary mixtures, where $c_i^{mixture}$ is the adsorbed loading of component i in the mixture calculated from GCMC simulations.

$$MAS_{(i/j)} = \frac{c_i^{mixture} / c_j^{mixture}}{y_i / y_j} \tag{4.7}$$

Ideal diffusion selectivity (IDS) of component i from component j is calculated as the ratio of single component self-diffusivities.

$$IDS_{(i/j)} = \frac{D_{i,self}^{pure}}{D_{j,self}^{pure}} \tag{4.8}$$

Mixture diffusion selectivity (MDS) of component i from component j is calculated as the ratio of self-diffusivities of species calculated in their binary mixtures.

$$MDS_{(i/j)} = \frac{D_{i,self}^{mixture}}{D_{j,self}^{mixture}} \tag{4.9}$$

After computing adsorption and diffusion selectivities, membrane selectivities of materials are predicted. Ideal membrane selectivity (IMS) of component i from component j is calculated as the multiplication of ideal adsorption selectivity and ideal diffusion selectivity.

$$IMS_{(i/j)} = IAS_{(i/j)} \times IDS_{(i/j)} \tag{4.10}$$

Similarly, mixture membrane selectivity (MMS) of component i from component j is calculated as the multiplication of mixture adsorption selectivity and mixture diffusion selectivity.

$$MMS_{(i/j)} = MAS_{(i/j)} \times MDS_{(i/j)} \tag{4.11}$$

Equations (4.9) and (4.10) require some assumptions. Membrane's selectivity is calculated at a given feed pressure, temperature and feed gas composition by assuming that permeate

side of the membrane is at vacuum. More details of this approximation and its validation by Keskin and Sholl can be found in an earlier study [81].

Some other parameters are also available to evaluate the separation performances of ZIF membranes. These following parameters are calculated by using mixture GCMC simulations data in this thesis. Working capacity (ΔN) is defined as the difference between the loading amounts of the gases and given in the unit of mol gas per kg of adsorbent at the corresponding adsorption and desorption pressures [19]:

$$\Delta N = N^{ads} - N^{des} \tag{4.12}$$

The adsorption pressure is fixed to 1 MPa, desorption pressure to 0.1 MPa and temperature to 298 K since several adsorption processes are performed under these conditions in the industry. Another important parameter is sorbent selection parameter (S_{sp}) which is the combination adsorption selectivity and working capacity. S_{sp} is an important parameter which compares the performances of different nanoporous materials in adsorption-based separation processes. Here subscripts 1 and 2 represent the strongly adsorbed component and the weakly adsorbed component, respectively [82]:

$$S_{sp} = \frac{(S_{ads(1/2)})^2}{S_{des(1/2)}} \times \frac{\Delta N_1}{\Delta N_2} \tag{4.13}$$

Last evaluation parameter used to evaluate separation performances of adsorbents is Regenerability (R(%)). Regenerability is the ratio of working capacity to the amount of adsorbed gas at the adsorption pressure and it is an important parameter to estimate the potential of an adsorbent for cyclic pressure-swing adsorption processes [82]:

$$R(\%) = \frac{\Delta N_1}{N_1^{ads}} \times 100 \tag{4.14}$$

In this thesis, graph of working capacity versus adsorption selectivity is used for quick determination of the performances of ZIFs at adsorption-based gas separation applications. A good adsorbent should have high adsorption selectivity due to the fact that the purity of the product increases by high selectivity. Additionally, high working capacity is also required for good adsorbent candidates because high working capacity demonstrates the storage capacity for the strongly adsorbed gas molecule in the mixture at working conditions. Also ZIFs should have high S_{sp} and R. The former one should be high since it gives information about combination of working capacity and adsorption selectivity. The latter gives idea about the efficiency of the adsorbent in an operation cycle.

In this study, the graph of permeability versus MMS is used for quick evaluation of the performances of ZIFs at membrane-based gas separation applications. A promising membrane should have high selectivity since it means the purity of the product to increase. Additionally, high permeability is also required due to the fact that it decreases the required amount of surface area. As surface area requirement decreases, less amount of ZIF can be used. Therefore, cost can be reduced. For a cost effective and efficient separation, a membrane should exhibit both high selectivity and permeability.

Chapter 5: Computational Screening of ZIFs for CO_2 Separations

This chapter focuses on a diverse collection of sixteen ZIFs and explores their performances in adsorption-based and membrane-based CO_2/CH_4, CO_2/N_2, CO_2/H_2 and CH_4/H_2 separations. The first information on selectivities of several ZIFs in adsorption and membrane-based separations using Grand Canonical Monte Carlo (GCMC) and equilibrium molecular dynamics (EMD) simulations [83]. These molecular simulations are performed for binary gas mixtures of CH_4/H_2, CO_2/CH_4, CO_2/H_2 and required a significant amount of computational time, especially for computing mixture self-diffusivities at various compositions. In this study, molecular simulations are performed for pure gases (CO_2, H_2, N_2 and CH_4) rather than mixtures and used the single component adsorption and diffusion data for predicting intrinsic selectivity (ideal selectivity) of ZIFs. Adsorption selectivity, diffusion selectivity and membrane selectivity of ZIFs calculated from single component data are then used to rapidly screen ZIFs for gaining large amounts of savings in computational time and cost. Then the selectivities calculated from single component data are compared with the selectivities calculated from computationally demanding mixture simulations of CO_2/CH_4, CO_2/N_2, CO_2/H_2, CH_4/H_2 and the importance of 'mixture effects' on making predictions about a material's separation performance is discussed. In addition to selectivities, gas permeability, working capacity and sorbent selection parameters of ZIFs are computed for each gas separation to identify the most promising materials in adsorption-based and membrane-based separations.

5.1. Molecular Simulations

Sixteen different materials are studied, ZIF-1, ZIF-2, ZIF-3, ZIF-6, ZIF-8, ZIF-10, ZIF-11, ZIF-12, ZIF-60, ZIF-65, ZIF-67, ZIF-69, ZIF-78, ZIF-79, ZIF-81 and ZIF-90 in this work. The atomic positions of ZIFs are taken from experimental X-ray diffraction (XRD) studies and solvent-free, rigid structures are used in all molecular simulations [30, 32, 34, 84]. All

molecular simulations are performed using universal force field (UFF) [71] because UFF fully defines the interatomic potentials needed for all ZIF atoms. Previous studies showed that the results of molecular simulations employing UFF agree well with the experimental measurements of gas permeances and permeabilities through ZIF membranes [73, 85].

Conventional grand canonical Monte Carlo (GCMC) simulations are employed to compute single component and mixture adsorption isotherms of gases in ZIFs. By specifying the temperature and fugacity of the adsorbing gases, the number of adsorbed molecules is calculated at equilibrium. Four types of trial moves, attempts to translate a molecule, attempts to rotate a molecule, attempts to create a new molecule and attempts to delete an existing molecule are included. A cut-off distance of 13 Å is used for LJ interactions and 25 Å is used for electrostatic interactions. Periodic boundary conditions are applied in all simulations. The size of the simulation box is increased up to 4×4×4 unit cells in cases to accommodate enough adsorbates to guarantee the simulation accuracy at the lowest loadings. Simulations at the lowest fugacity for each system are started from an empty ZIF matrix and each subsequent simulation at higher fugacity is started from the final configuration of the previous run. Simulations included minimum 1.5×10^7 cycle equilibration period followed by a 1.5×10^7 cycle production run.

Single component and mixture self-diffusivities are computed using equilibrium molecular dynamics (EMD) simulations in the canonical ensemble with a Nosé-Hoover thermostat [54]. After creating initial states with the appropriate loadings using GCMC, each system is equilibrated with EMD for about 20 ps prior to taking data. Ten independent EMD simulations are performed to compute single component and mixture self-diffusivities of gases. More details of using EMD simulations to obtain various diffusion coefficients can be found in previous studies of zeolites, carbon nanotubes, MOFs and ZIFs [86-88]. In mixture EMD simulations, the compositions of the gas mixtures are set to compute the self-diffusivity of the less adsorbed component with a high statistical accuracy. The compositions are set as: CO_2/CH_4:10/90, CO_2/N_2:15/85, CO_2/H_2:1/99 and CH_4/H_2:10/90. All molecular simulations are performed at room temperature unless otherwise specified.

5.2. Adsorption-based Separation Performance of ZIFs

Three different types of selectivity are defined to examine the efficiency of ZIFs in an adsorption-based separation process: ideal adsorption selectivity (IAS) which is the ratio of adsorbed amounts of single-component gases, composition-based adsorption selectivity

(CBAS) which is the ratio of adsorbed amounts of single-component gases at their partial pressures corresponding to mixture cases and mixture adsorption selectivity (MAS) which is the ratio of adsorbed amounts of gases in binary mixtures. Firstly, experimentally reported IAS values are collected for several ZIFs from the literature and compared our calculated IAS values with the experimental ones to validate the accuracy of our molecular simulations. The good agreement between experimental measurements and our simulation results can be seen in Figure 5.1.

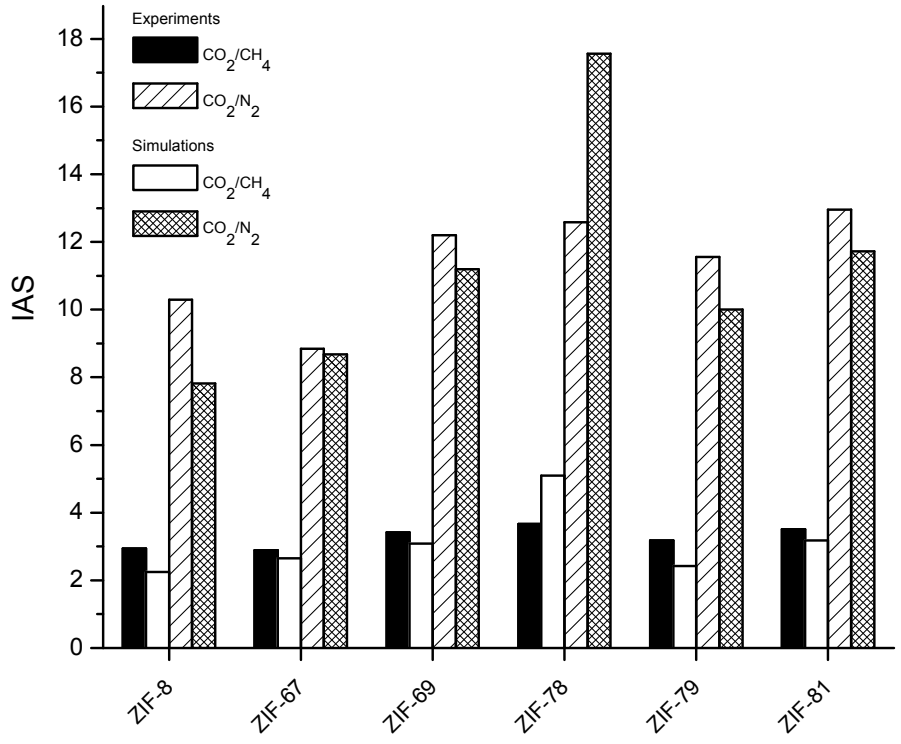

Figure 5.1. Comparison of IAS results computed from simulations and experimental measurements [34, 89, 90] for ZIF-8, ZIF-67, ZIF-69, ZIF-78, ZIF-79 and ZIF-81 at 298 K and 1 bar.

IAS, CBAS and MAS of each ZIF for CO_2/CH_4, CO_2/N_2, CO_2/H_2 and CH_4/H_2 separations are calculated and the results for CO_2/CH_4 are showed in Figure 5.2. Graphs for the other mixtures can be found in Figures A1-A3 in Appendix A. Since there is no experimental data for MAS or CBAS in the literature, comparison for these selectivities could not be made. Figure 5.2 demonstrates that general trend is CBAS>MAS>IAS for CO_2/CH_4 separations. Since there is no experimental data for CBAS or MAS in the literature, it could not be

possible any comparison between simulation results and experiments for these selectivities. The trend can be explained with the following discussion: The amount of adsorbed CO_2 in CO_2/CH_4:10/90 mixture at 10 bar (partial pressure of CO_2 is 1 bar) is less than the amount of single-component CO_2 adsorbed at 1 bar. Therefore, CBAS is expected to be higher than MAS. One exception to this is ZIF-78, for which MAS is significantly higher than CBAS. High MAS of ZIF-78 is attributed to the strong CO_2 adsorption over CH_4 in CO2/CH_4 mixtures. In order to understand this, CO_2/CH_4 mixture adsorption isotherms of ZIF-78 with ZIF-79, two ZIFs which have the same topology but different functional groups, are compared. Figure 5.3(a) shows the single-component and binary mixture adsorption isotherms of CO_2 and CH_4 in ZIF-79. As discussed before, adsorbed amount of CO_2 decreases significantly in the mixture compared to single-component case and therefore CBAS becomes greater than MAS. On the other hand, Figure 5.3(b) shows that the amount of adsorbed CO_2 in ZIF-78 is significantly larger than the amount of adsorbed CH_4 even though the composition of the feed mixture is very CH_4 dominant (CO_2/CH_4:10/90). This high CO_2 affinity of ZIF-78 is explained by the existence of highly polar -NO_2 functional groups in the framework which causes strong electrostatic interactions between CO_2 and ZIF-78 as discussed in the literature before [34].

Table 5.1 compares MAS of ZIFs with well-known zeolites and metal organic frameworks (MOFs) for CO_2/CH_4, CO_2/N_2, CO_2/H_2 and CH_4/H_2 separations under the same operating conditions (298 K, 10 bar). Results show that ZIFs are promising adsorbents especially in CO_2 separations due to their high CO_2 selectivity compared to traditional zeolites MFI, ITQ-29 and widely studied MOFs, CuBTC, IRMOF-1. ZIF-78 is a promising adsorbent candidate with high MAS values for all the gas separations considered. One important point to note is that none of the ZIFs studied in this work can outperform the CO_2 separation performance of NaX and NaY which have very high CO_2 selectivities due to the strong electrostatic interaction between CO_2 and nonframework cations (Na^+) of these materials [19]. However, molecular simulations demonstrate the drawbacks of these adsorbents, very low working capacities [19].

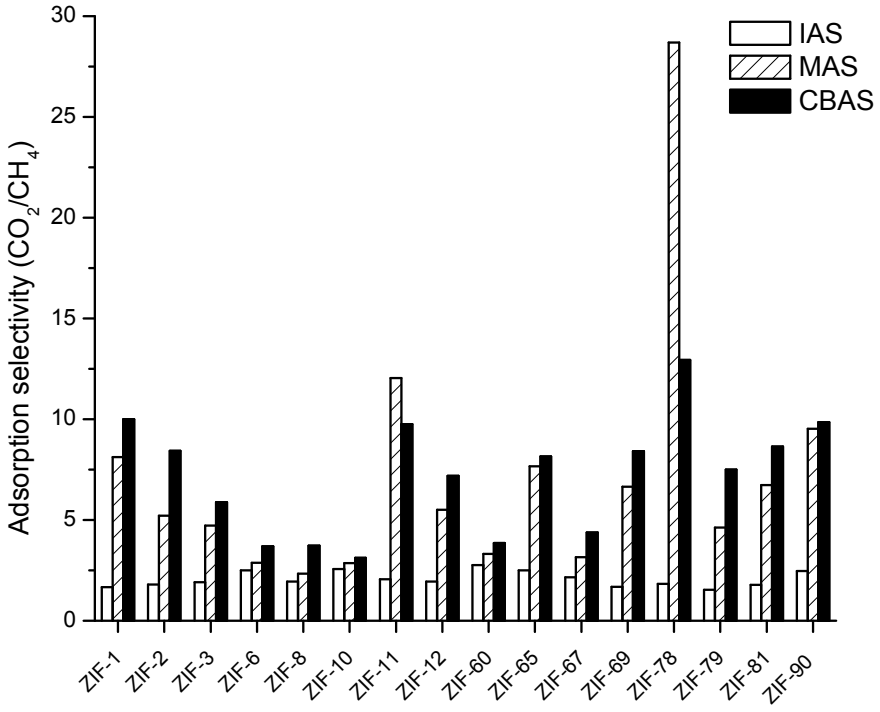

Figure 5.2. Adsorption selectivity of ZIFs for CO_2 in CO_2/CH_4 separations at 298 K and 10 bar. The compositions of bulk gas mixtures are CO_2/CH_4:10/90.

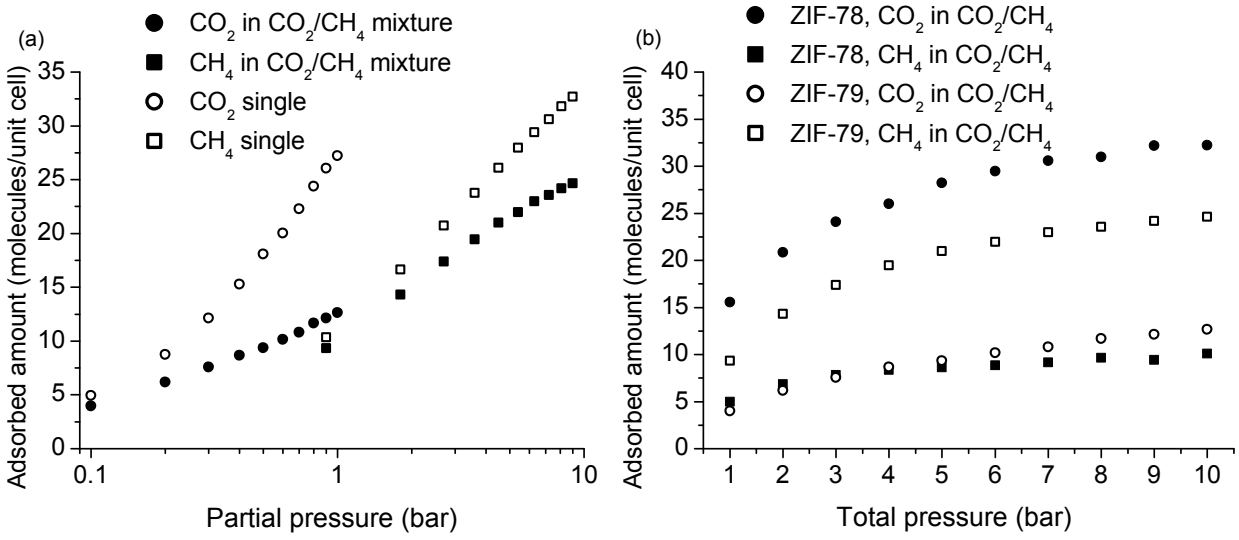

Figure 5.3.(a)Single component and binary mixture adsorption of CO_2 and CH_4 in ZIF-79 at corresponding partial pressures, (b)binary mixture adsorption isotherms of CO_2 and CH_4.

The composition of the bulk mixture is 10% CO_2 and 90% CH_4 and total pressure is from 1 to 10bar at 298K.

Table 5.1 MAS of ZIFs, MOFs and zeolites for CO_2/CH_4, CO_2/N_2, CO_2/H_2 and CH_4/H_2 separations.

Materials	CO_2/CH_4	Materials	CO_2/H_2	Materials	CO_2/N_2	Materials	CH_4/H_2
NaX	44.64	NaX	1440.51	NaX	2686.54	ZIF-1	63.48
NaY	29.06	ZIF-78	1115.13	NaY	532.83	ZIF-79	52.17
ZIF-78	28.69	NaY	530.62	AFX	295.34	ZIF-81	40.09
CHA	15.53	AFX	508.67	ZIF-78	152.83	ZIF-78	39.43
ZIF-11	12.05	ZIF-11	431.91	MgMOF-74	53.43	ZIF-69	39.23
MgMOF-74	11.84	ZIF-1	364.86	ZIF-1	46.56	ZIF-11	36.30
ZIF-90	9.53	MgMOF-74	306.39	CHA	45.03	ZIF-12	34.71
ZIF-1	8.12	ZIF-69	240.07	ZIF-11	40.02	ZIF-2	33.01
ZIF-65	7.67	ZIF-81	235.91	DDR	32.62	ZIF-3	29.06
ZIF-81	6.73	ZIF-12	196.10	ZIF-69	30.72	ZIF-8	20.92
ZIF-69	6.64	ZIF-79	195.94	ZIF-81	29.90	ZIF-67	20.82
ZnMOF-74	6.08	ZIF-3	176.43	ZIF-90	28.68	MgMOF-74	19.58
ZIF-12	5.51	ZIF-2	160.87	ZIF-65	24.59	ZnMOF-74	19.53
ZIF-2	5.22	ZIF-90	137.44	ZIF-79	23.81	ZIF-90	15.16
ZIF-3	4.73	CHA	115.95	ZIF-12	21.86	ZIF-65	14.37
ZIF-79	4.62	ZnMOF-74	108.83	ZnMOF-74	20.52	ZIF-6	13.69
DDR	4.52	ZIF-65	102.08	ZIF-2	18.37	CHA	12.42
CuBTC	4.10	MFI	93.87	ZIF-3	16.13	ZIF-10	11.05
ZIF-60	3.32	DDR	49.81	MFI	14.16	ZIF-60	10.93
ZIF-67	3.15	CuBTC	47.75	CuBTC	12.61	ITQ-29	8.28
MFI	2.99	ZIF-67	43.48	ZIF-67	11.56	LTA-Si	6.45
ZIF-6	2.87	ZIF-8	34.89	ZIF-60	9.68	MOF-177	4.68
ZIF-10	2.86	ZIF-6	34.68	ZIF-8	8.62	CuBTT	4.34
ITQ-29	2.77	ZIF-60	31.21	ZIF-6	8.59		
ZIF-8	2.34	ZIF-10	27.55	ZIF-10	7.75		
IRMOF-1	1.99	ITQ-29	20.51	MOF-177	4.77		

Data for MOFs and zeolites are taken from the literature [19]. The bulk composition of CO_2/CH_4, CO_2/H_2, CO_2/N_2 and CH_4/H_2 mixtures are 10/90 (50/50), 1/99 (15/85), 15/85 (15/85) and 10/90 (50/50) for ZIFs (MOFs and zeolites) at 298 K (300 K) and 10 bar.

High working capacity is another crucial property which is as desirable as high adsorption selectivity for an economic adsorption-based separation process. Figure 5.4 shows that CO_2 working capacities of ZIFs are higher than many other MOFs such as amine-MIL-53(Al), HKUST-1 and zeolite-13X in CO_2/CH_4 separation. The CO_2 working capacities calculated for CO_2/H_2 separation are a lot lower than the CO_2 working capacities calculated for CO_2/N_2 and CO_2/CH_4 separations since the partial pressure of CO_2 is very low under the composition considered for this mixture (CO_2/H_2:1/99). It is important to mention why the composition of this mixture is set to this value: In this work, membrane selectivities of ZIFs are calculated using diffusion selectivities obtained from EMD simulations. The adsorbed mixture is very

CO_2 dominant in CO_2/H_2 mixtures and it is statistically not accurate to measure mixture self-diffusivities when one of the components is very strongly adsorbed. Therefore, mixture EMD simulations are performed at a bulk gas composition of CO_2/H_2:1/99 to get statistically accurate diffusion results. Working capacity graphs are given for CO_2/CH_4 and CO_2/H_2 mixtures and the graphs for other mixtures are presented in Figures A4 and A5 (See Appendix A).

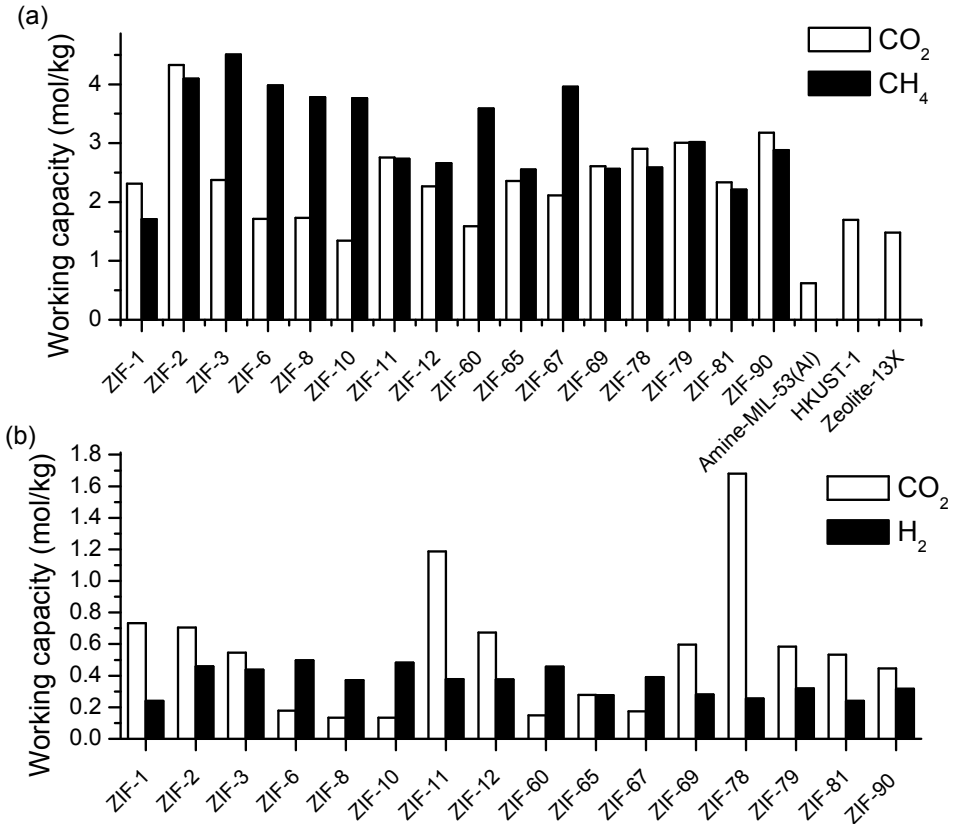

Figure 5.4. Working capacity of ZIFs for CO_2, CH_4, in H_2 (a) CO_2/CH_4 (10/90), (b) CO_2/H_2 (1/99) in 298 K. Adsorption and desorption pressures are 10 and 1 bar, respectively. Data for amine-MIL-53 (Al), HKUST-1 and zeolite-13X is taken from Reference [82].

The results in Figure 5.4 suggest that materials exhibiting high CO_2 working capacity may have low adsorption selectivity for CO_2, such as ZIF-2. In order to evaluate the trade-off between adsorption selectivity and working capacity, Bae et al. [82] introduced the sorbent selection parameter (S_{sp}). Sorbent selection parameter is useful to evaluate the potential of an adsorbent material by considering both the adsorption selectivity and working capacity. Bae et al. [82] calculated S_{sp} values of three ZIFs, ZIF-78, ZIF-79, ZIF-81 and the values for same materials are compared in Table 5.2. Slight differences between these S_{sp} values can be attributed to the different evaluation techniques: Bae et al. [82] did not perform simulations and used only experimental data in their S_{sp} calculations whereas S_{sp} values are calculated

using molecular simulations without any experimental input. In fact, the good agreement between two sets of results also validates the accuracy of our molecular simulations. S_{sp} values of all ZIFs that are considered in this study are presented for all gas separations in Figure 5.5. ZIF-1, ZIF-65, ZIF-78, ZIF-79 are the best adsorbent candidates with the highest S_{sp} values for CO_2/CH_4, CO_2/N_2, CO_2/H_2 and CH_4/H_2 separations, respectively.

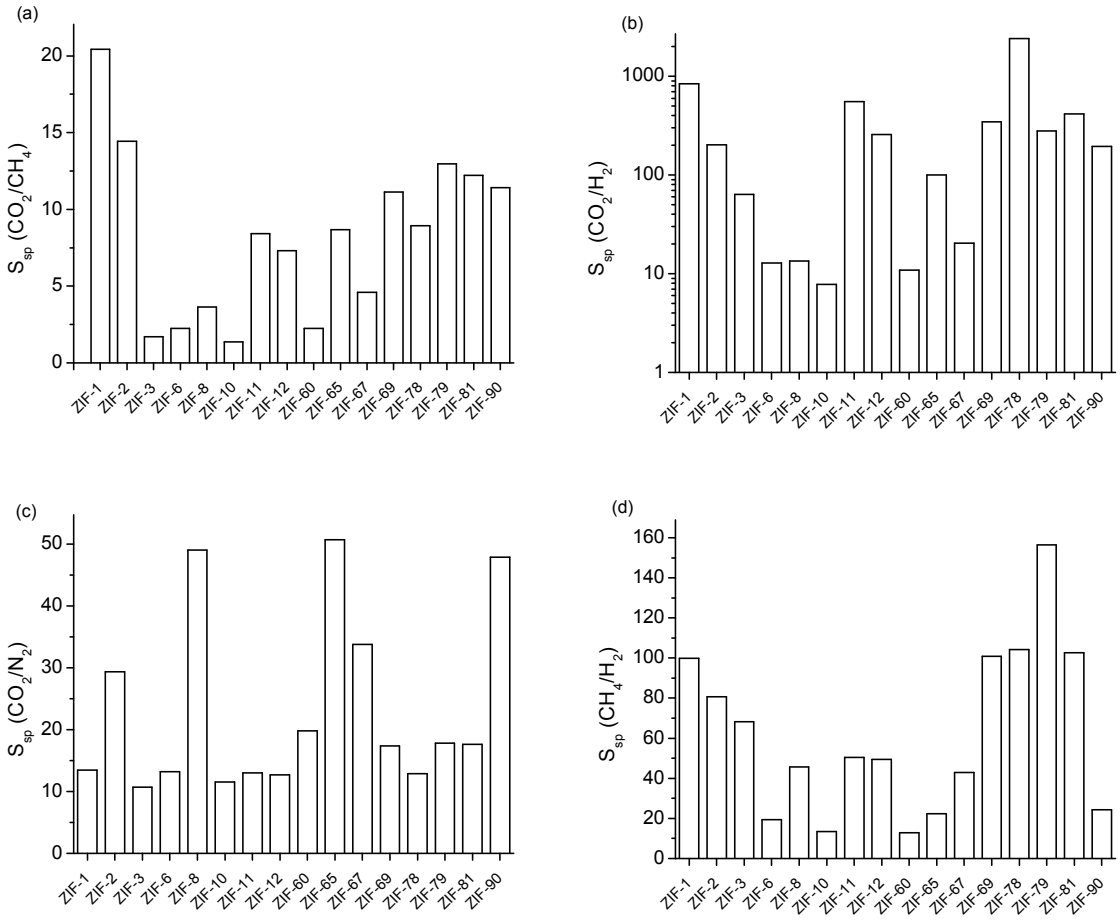

Figure 5.5. S_{sp} values of ZIFs for (a) CO_2/CH_4 (10/90), (b) CO_2/H_2 (1/99), (c) CO_2/N_2 (15/85) and (d) CH_4/H_2 (10/90) at 298 K. Adsorption and desorption pressures are 10 and 1 bar, respectively. Data for amine-MIL-53 (Al), HKUST-1 and zeolite-13X is taken from Reference [82].

Table 5.2 Comparison of S_{sp} values calculated from our molecular simulations with the results of Bae et al. [82] for equimolar CO_2/CH_4 at 298 K. Adsorption and desorption pressures are set to 1 bar and 0.1 bar, respectively.

	Bae et al. [82]	**This work**
ZIF-78	10	16
ZIF-79	8	5
ZIF-81	6	9

5.3. Membrane-based Separation Performances of ZIFs

Evaluating the membrane-based separation performance of ZIFs requires information about the transport of gases in ZIFs' pores. Both the single-component and mixture diffusivities of gases are computed and showed ideal diffusion selectivity (IDS) and mixture diffusion selectivity (MDS) of ZIFs in Figure 5.6. The values of IDS and MDS are generally close to each other for all ZIFs and all gas mixtures. When the diffusion rates of gases in ZIFs are considered, CO_2 and H_2 represent the slowest and fastest gas molecules. Figure 5.6 shows that MDS for CO_2 is generally higher than IDS. This can be explained with the following discussion: Single-component diffusivity of CO_2 is less than the diffusivity of H_2. However, when CO_2 and H_2 molecules are together in mixtures, fast diffusing H_2 molecules get slower and slow diffusing CO_2 molecules get faster due to momentum exchange of different species, also known as 'mixture effects'. The observation that a slowly diffusing species strongly reduces the diffusivity of a faster diffusing species in an adsorbed mixture is a very common one [91]. Another important observation from this figure is that IDS and MDS favor H_2 (IDS, MDS<1) since CO_2 always diffuses slower than H_2 both in single-component and mixture cases. CO_2/H_2 separation is an example where adsorption (IAS and MAS) strongly favors CO_2 whereas diffusion (IDS and MDS) favors the less adsorbed component, H_2. This type of systems does not yield high membrane selectivity since adsorption and diffusion compensate each other. In Figure 5.6, CO_2/H_2 and CO_2/CH_4 mixture are represented. The diffusion selectivity graphs of other mixtures are given in Figures A6 and A7 (See Appendix A).

Using adsorption and diffusion selectivities, membrane selectivity of a material can be predicted. Ideal membrane selectivity (IMS) is calculated based on single-component adsorption and diffusion data whereas mixture membrane selectivity (MMS) is calculated using mixture adsorption and diffusion data for CO_2/CH_4, CO_2/N_2, CO_2/H_2 and CH_4/H_2 separations. MMS includes mixture effects such as competition for adsorption and change in diffusion rates of gas species as discussed earlier. IMS and MMS predictions are represented for all ZIFs for CO_2/CH_4 (10/90) and CO_2/H_2 (1/99) in Figure 5.7 (See Figures A8 and A9 for CO_2/N_2 and CH_4/H_2 in Appendix A). MMS values are always found to be higher than IMS values for all ZIFs and for all gas separations. Previously, it is showed that MDS of ZIFs are either less than or similar to IDS whereas MAS of ZIFs is a lot higher than IAS. As a result, MMS becomes higher than IMS.

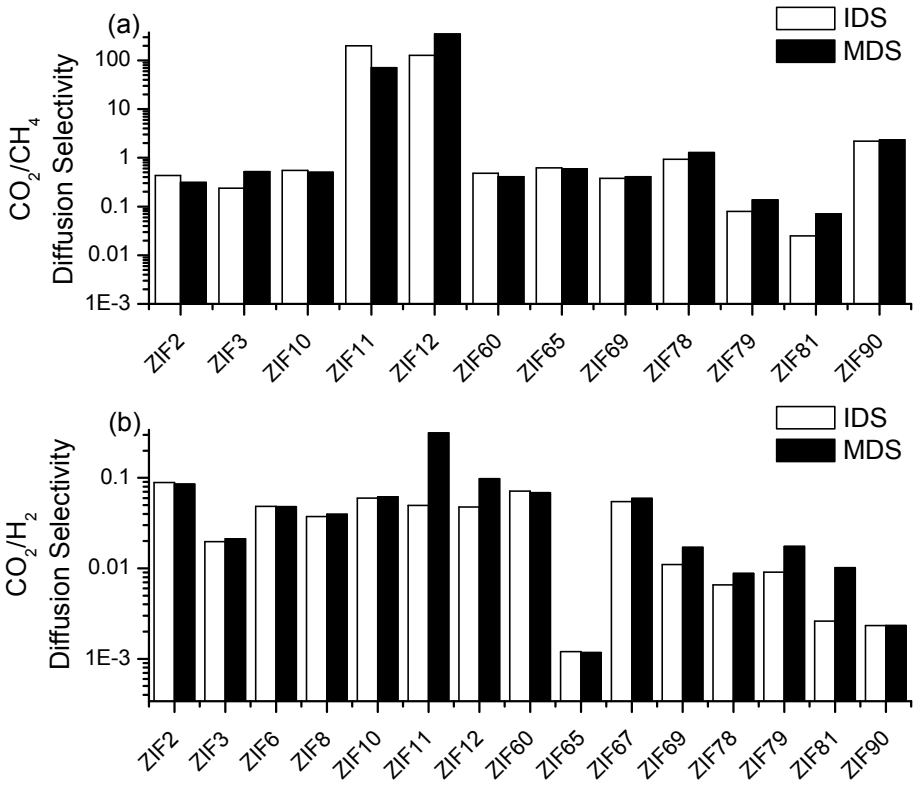

Figure 5.6. Diffusion selectivity of ZIFs for CO_2, CH_4, in H_2 (a) CO_2/CH_4 (10/90), (b) CO_2/H_2 (1/99) at 298 K and 10 bar.

Another important observation is that MAS values are higher than MMS values for most of the ZIFs. This observation highlights the fact that MAS is compensated by the low MDS since strongly adsorbed species diffuse more slowly than the weakly adsorbed species [81]. Examples of ZIFs where gas adsorption and diffusion do not compensate each other would be very interesting because these ZIFs will perform highly selective both as adsorbents and membranes. For example, MMS of ZIF-8, ZIF-11, ZIF-12 and ZIF-67 for CO_2/N_2 separation are higher than their MAS because both adsorption and diffusion favor CO_2. It would be expected to see a lower diffusion coefficient for CO_2 compared with N_2 but diffusion of N_2 is found to be slow (10^{-7}-10^{-8} cm^2/s) in these ZIFs since the narrow pore size (3.4 Å) of these ZIFs is similar to the kinetic diameter of N_2 (3.3 Å).

Figure 5.7 also emphasizes the importance of why it may be important to characterize the membranes based on their performance for mixed gas feeds, not merely to extrapolate their performance from single-component gas studies, at least for some gas pairs. For example, IMS calculated using single-component gas data suggests that ZIF-69 is not a selective membrane with a CO_2 selectivity of 0.9 for CO_2/N_2 separation whereas MMS calculated using mixture data suggests that ZIF-69 is a promising membrane material with a good CO_2/N_2

selectivity of 12.8. This result shows that although it is widely used in the literature, ideal selectivity may give misleading information about a membrane's separation performance in some cases. In Table 5.3, the MMS of ZIFs are compared with other nanoporous materials and concluded that ZIF-11, ZIF-12 and ZIF-78 are very promising membrane materials for CO_2 separation compared with other nanoporous materials. These ZIFs exhibit higher selectivity than the widely studied zeolites and MOFs such as DDR, CHA, MFI, CuBTC and MOF-177.

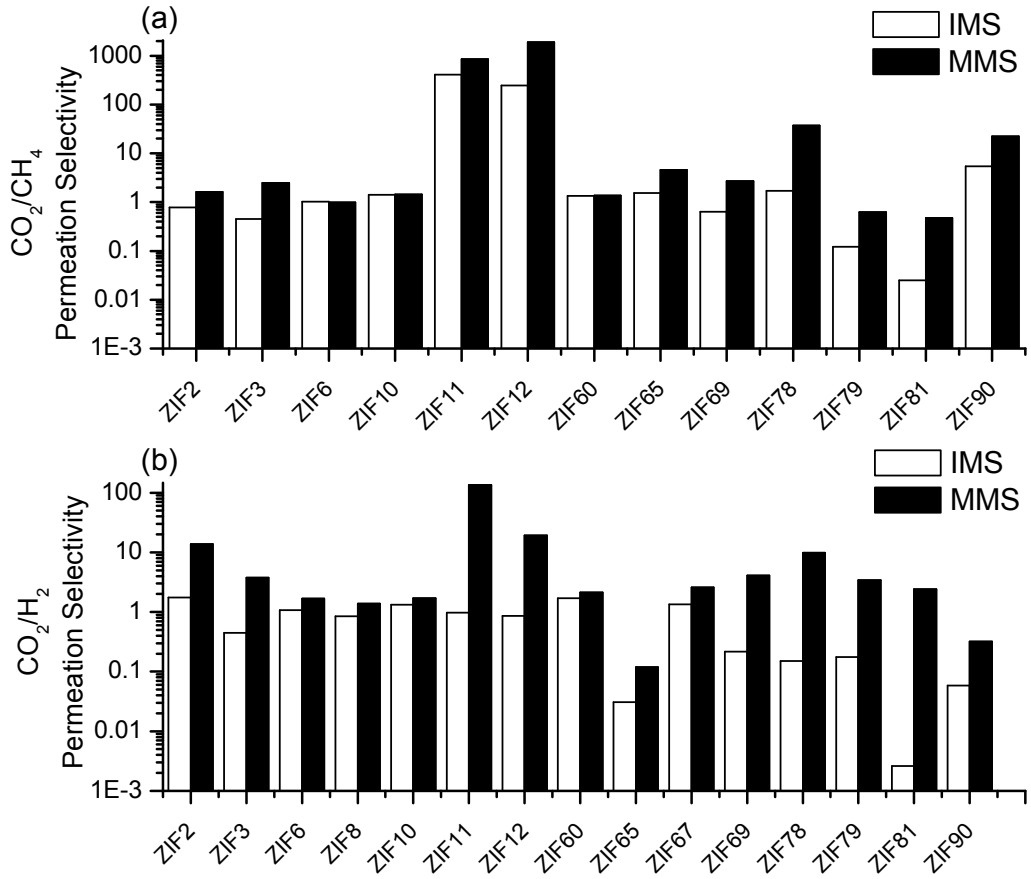

Figure 5.7. Permeation selectivity of ZIFs for CO_2, CH_4, in H_2 (a) CO_2/CH_4 (10/90), (b) CO_2/H_2 (1/99) at 298 K and 10 bar.

In any effort to use molecular modeling in studying performances of materials, the assumptions associated with modeling methods should be clearly stated to allow judgments to be made about the potential impact of these factors in the real-world performance of materials. Almost all of the molecular simulations for MOFs and ZIFs in the literature used rigid framework assumption because it saves a significant amount of computational time, and molecular simulations should be performed for multiple materials on time scales shorter

than the same materials can be assessed experimentally. Since adsorption involves low energy equilibrium configurations, the flexibility of the framework has a marginal effect on the adsorption of gas molecules [47].

Table 5.3 MMS of ZIFs, MOFs and zeolites for CO_2/CH_4, CO_2/H_2, CO_2/N_2 and CH_4/H_2 separations.

Materials	CO_2/CH_4	Materials	CO_2/H_2	Materials	CO_2/N_2	Materials	CH_4/H_2
ZIF-12	1913.32	ZIF-11	136.08	ZIF-12	1801.58	ZIF-2	10.62
ZIF-11	849.05	NaX	60.41	NaX	676.64	ZIF-79	9.18
DDR	140.26	NaY	51.60	ZIF-67	437.62	ZIF-81	6.77
CHA	135.77	MgMOF-74	30.17	ZIF-11	348.76	ZnMOF-74	5.23
ZIF-78	36.86	ZIF-12	19.19	NaY	220.06	MgMOF-74	4.09
ZIF-90	22.29	ZnMOF-74	15.39	ZIF-8	187.03	ZIF-3	3.00
NaY	20.77	ZIF-2	13.70	ZIF-78	81.65	ZIF-69	2.41
NaX	19.35	MFI	12.87	CHA	37.65	ZIF-6	2.19
MgMOF-74	4.61	ZIF-78	9.80	DDR	20.38	CuBTT	2.08
ZIF-65	4.56	CHA	8.10	MgMOF-74	17.94	ZIF-60	1.73
ZnMOF-74	3.92	DDR	7.85	ZIF-69	12.86	ZIF-10	1.65
ZIF-69	2.71	ZIF-3	4.31	ZnMOF-74	9.45	MOF-177	0.89
ZIF-3	2.46	ZIF-69	4.09	MFI	9.24	ZIF-78	0.48
MFI	2.35	ZIF-79	3.41	ZIF-2	8.53	ZIF-11	0.09
CuBTC	2.00	ZIF-67	2.59	CuBTC	4.46	LTA-Si	0.06
ZIF-2	1.63	CuBTC	2.55	ZIF-60	3.92	ZIF-12	0.06
ZIF-10	1.44	ZIF-81	2.41	ZIF-79	3.38	ZIF-65	0.03
ZIF-60	1.36	ZIF-60	2.14	ZIF-65	3.34	ZIF-90	0.02
MOF-177	1.29	ZIF-10	1.70	ZIF-10	2.97	CHA	0.01
ZIF-6	0.98	ZIF-6	1.67	ZIF-6	2.41	ITQ-29	0.01
ZIF-79	0.63	ZIF-8	1.39	MOF-177	2.12		
ZIF-81	0.47	MOF-177	0.84	ZIF-81	1.59		
		ZIF-90	0.32	ZIF-3	1.59		
		ZIF-65	0.12	ZIF-90	0.86		

Data for MOFs and zeolites are taken from the literature [19]. The bulk composition of CO_2/CH_4, CO_2/H_2, CO_2/N_2 and CH_4/H_2 mixtures are 10/90 (50/50), 1/99 (15/85), 15/85 (15/85) and 10/90 (50/50) for ZIFs (MOFs and zeolites) at 298 K (300 K) and 10 bar.

Chapter 6: Analysis of Effects of Molecular Simulation Parameters

In this chapter, gas separation potentials of two ZIFs, ZIF-68 and ZIF-69 are examined. The effects of molecular simulation parameters on predicting gas separation performances of these ZIFs are analyzed.

6.1. ZIFs and Common Force Fields for ZIFs

ZIF-68 and ZIF-69 are chemically and thermally stable even at high temperatures which make them potential candidates for gas separation applications [30]. Both structures are hexagonal with the same primitive GME topology with Zn metal centers linked by different imidazolate linkers. ZIF-68 has benzimidazole (bIM) and 2-nitroimidazole (nIM) as the linkers while ZIF-69 contains 5-chlorobenzimidazole (cbIM) and 2-nitroimidazole (nIM). Crystal structures of ZIF-68 and ZIF-69 are constructed from their corresponding experimental X-ray diffraction [30]. Figures of crystal structures of ZIF-68 and ZIF-69 are given in Figures B1 and B2 in Appendix B. In order to understand the effect of FF parameters on the predicted separation performance of ZIFs, the molecular simulations are repeated using three different FFs for the LJ parameters of ZIFs: UFF, DREIDING, and the FF developed by Liu and Smit [39] which is referred as Liu FF throughout this chapter. As discussed above, several molecular simulation studies in the literature have used UFF parameters to calculate gas adsorption in ZIFs [40, 48, 52, 92]. Atci and Keskin [73] recently showed that predictions of UFF-based simulations agree well with the experimental gas permeance data of pure ZIF-90 membranes and ZIF-90-based mixed matrix membranes. DREIDING is the second widely used generic FF to compute gas adsorption and diffusion in ZIFs [93-95]. Liu and Smit [39] refined the UFF parameters and showed that the adsorption isotherms of CH_4, CO_2 and N_2 in ZIF-68 and ZIF-69 calculated by their new FF are in a much better agreement with the experimentally measured adsorption isotherms. Therefore, we computed the LJ interactions

between ZIF atoms and gases using these three FFs. In order to compute the electrostatic interactions between the ZIF atoms and gases that have quadrupole moments (CO_2 and N_2), partial atomic charges are assigned to ZIF atoms. The framework charges are taken from the Density Functional Theory (DFT) calculations of ZIF-68 and ZIF-69 [39, 40].

6.2. Molecular Simulations

Grand canonical Monte Carlo (GCMC) and Equilibrium Molecular Dynamics (EMD) simulations are used to compute adsorption, diffusion and separation properties of ZIF-68 and ZIF-69 for CH_4/H_2, CH_4/N_2, CO_2/CH_4, CO_2/H_2 and CO_2/N_2 mixtures. Single-component (CH_4, CO_2, N_2 and H_2) and mixture adsorption isotherms (CH_4/H_2, CH_4/N_2, CO_2/CH_4, CO_2/H_2 and CO_2/N_2) are obtained from the GCMC simulations. The interactions between the gases and ZIF frameworks in GCMC simulations are modeled using LJ potential. Electrostatic interactions between the framework atoms and gases are computed using Coulomb potential. The Lorentz-Berthelot mixing rules are employed and the cut-off distance for truncation of the intermolecular (electrostatic) interactions is set to 13 (25) Å. Periodic boundary conditions are applied in all simulations. For GCMC, a simulation box of 2×2×2 crystallographic unit cells is used. During the simulations, 1.5×10^7 steps are performed to guarantee the equilibration and 1.5×10^7 steps are performed to sample the desired properties. EMD simulations are performed to compute mixture self-diffusivities (CH_4/H_2, CH_4/N_2, CO_2/CH_4, CO_2/H_2 and CO_2/N_2). The initial states of EMD simulations with the appropriate gas loadings are taken from the GCMC simulations and each system is equilibrated for 20 ps prior to taking data. At the lowest gas loadings, the size of the simulation volume is increased up to 4×3×3 to contain enough particles during the EMD simulations. Twenty independent EMD simulations with a length of 16 ns are performed to compute diffusivities of gases at a given loading. The Nosé-Hoover thermostat is applied in EMD simulations at NVT ensemble. More details of GCMC and EMD simulations can be found in our earlier studies [96, 97].

6.3. Comparison of Experimental and Simulated Results

In this work, the aim is to examine the effect of FF parameters used in molecular simulations on the predicted gas separation performance of ZIF adsorbents and membranes. Experimental data is available for single-component adsorption of CH_4, CO_2, N_2, H_2 in ZIF-68 and CH_4, CO_2, N_2 in ZIF-69 [34, 47]. Therefore, firstly comparison is made between excess gas uptake results which are obtained from simulations using different FFs with the

experimental data in Figures 6.1 and 6.2 for ZIF-68 and ZIF-69, respectively. The simulation results based on UFF and DREIDING overestimated the experimental adsorption isotherms at 273 K for all gases in ZIF-68 and ZIF-69. Liu and Smit [39] previously reported this overestimation and described the Liu FF by modifying the UFF parameters to get a better agreement with the experiments. Therefore, Liu FF is used to calculate the excess gas uptake of ZIFs and found a good agreement between experiments and simulations for CH_4, CO_2 and N_2. However, estimations of Liu FF for H_2 did not agree well with the experimental data at low temperature, 77 K. In fact, Figure 6.1(d) suggests that simulations based on DREIDING make a better prediction for H_2 adsorption in ZIF-68 at 77 K. This comparison is only done at 77 K since there is not experimental H_2 adsorption data for ZIF-68 at 273 K in the literature.

One interesting observation from Table B1 in the Appendix B is that different research groups used different FFs for ZIFs and gas molecules to match their simulation results with the experiments. For example, Zhong's group [40] simulated CO_2 adsorption in ZIF-68 and ZIF-69 using UFF parameters without any modification and showed a good agreement with the experimental data as can be seen from Figures 6.1(b) and 6.2(b). This is due to the different CO_2 model that they used in their molecular simulations. They used a different set of LJ parameters and atomic partial charges for CO_2 (See Table B1) therefore, their simulation results agree well with the experiments even though they used UFF for ZIFs. On the other hand, Sirjoosingh et al. [48] used UFF for ZIFs and CO_2 molecules and their simulation results slightly overestimated the experimental results for ZIF-68 and ZIF-69. In fact, all these results suggest that combination of different FF parameters for gases and ZIFs may result in good agreements with the experiments and it is important to choose the appropriate FF not only for the ZIFs but also for the gas molecules.

Simulation results for gas uptakes are compared with the experiments at 298 K since gas separation properties of ZIFs (selectivity, working capacity, permeability) at room temperature to reflect the industrial operating conditions. Simulations based on Liu FF agree well with the experiments at this temperature whereas simulations based on UFF and DREIDING again overestimate the experimental adsorption isotherms measured at room temperature and it can be seen in Figures B3 and B4 in Appendix B. At both temperatures (273 and 298 K), single-component gas adsorption amounts of ZIF-68 and ZIF-69 are as following: CO_2>CH_4>N_2>H_2. CO_2 is the most strongly adsorbed molecule since it has three interaction sites and quadruple moment that causes additional electrostatic interactions with

the framework atoms. H_2, on the other hand, has the weakest interactions with the framework atoms and adsorption affinity of ZIFs for H_2 is very low compared to other gases. For example, at 0.1 MPa and 273 K, Liu FF predicts CO_2 (CH_4) adsorption in ZIF-68 and ZIF-69 as 3.36 (0.87) mmol/g and 3.80 (1.09) mmol/g, respectively. The uptake values for N_2 and H_2 are pretty low, N_2 (H_2) adsorption in ZIF-68 and ZIF-69 are estimated as 0.21 (0.009) mmol/g and 0.25 (0.008) mmol/g, respectively at the same conditions.

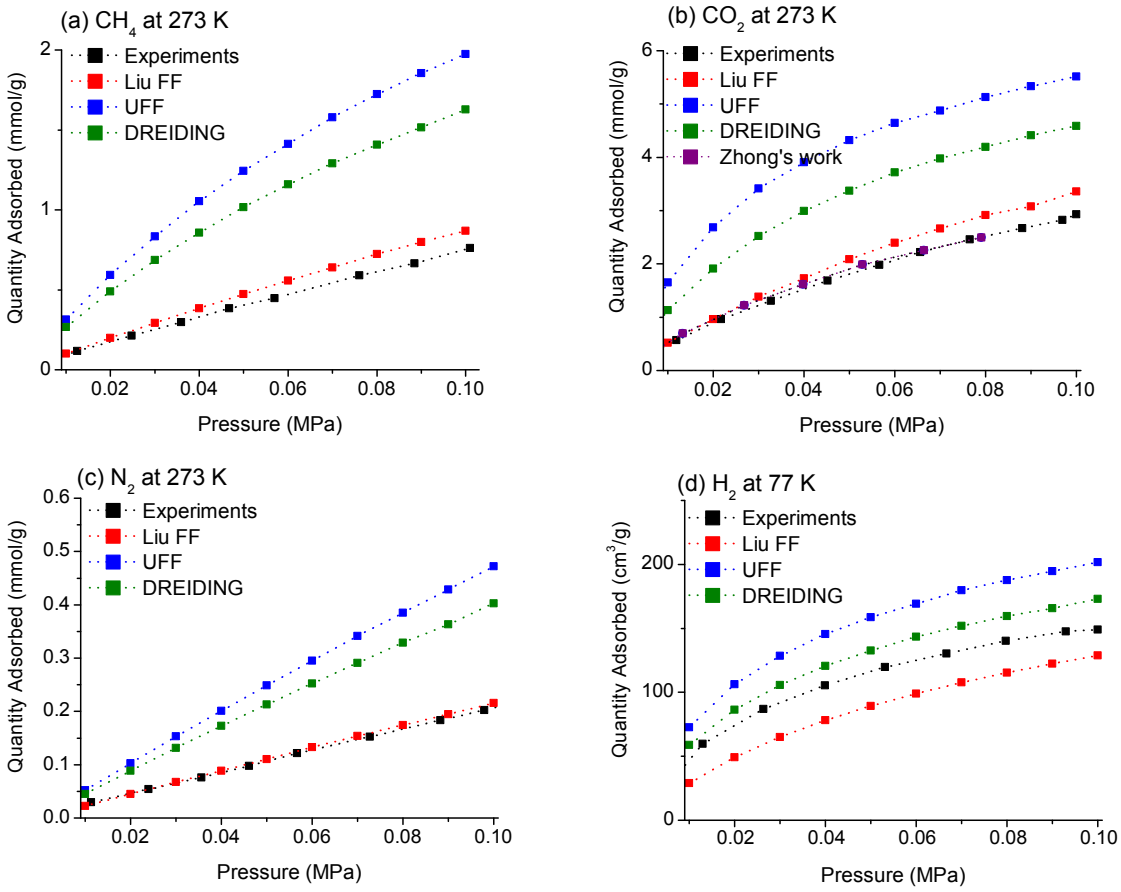

Figure 6.1. Comparison of experiments [34, 47] and molecular simulation results for single-component adsorption isotherms of (a)CH_4, (b)CO_2, (c)N_2 at 273 K, (d)H_2 at 77 K in ZIF-68. The CO_2 simulation results of Zhong's group [40] are also included in (b).

The gas uptake capacity of ZIF-69 is found to be higher than ZIF-68 at low pressure range, 0.001-0.5 MPa. For example, simulations based on Liu FF estimated the CO_2 uptake of ZIF-69 as 0.75 mmol/g at 0.01 MPa, 273 K whereas this value is 0.52 mmol/g in ZIF-68. This can be attributed to the additional cbIM linker of ZIF-69 that enhances the binding energy of CO_2 and increases its adsorption. The presence of Cl atoms in cbIM linker of ZIF-69, which are absent in ZIF-68, causes strong electrostatic interactions with CO_2 molecules [40]. At high

pressure range, ZIF-68 shows a higher CO_2 uptake capacity (8.35 mmol/g at 3 MPa) than ZIF-69 (6.75 mmol/g at 3 MPa). This is due to the dominance of entropic effects at high pressures. Since ZIF-68 has a higher pore volume and surface area than ZIF-69 adsorption of CO_2 is more preferred in ZIF-68 at high pressures.

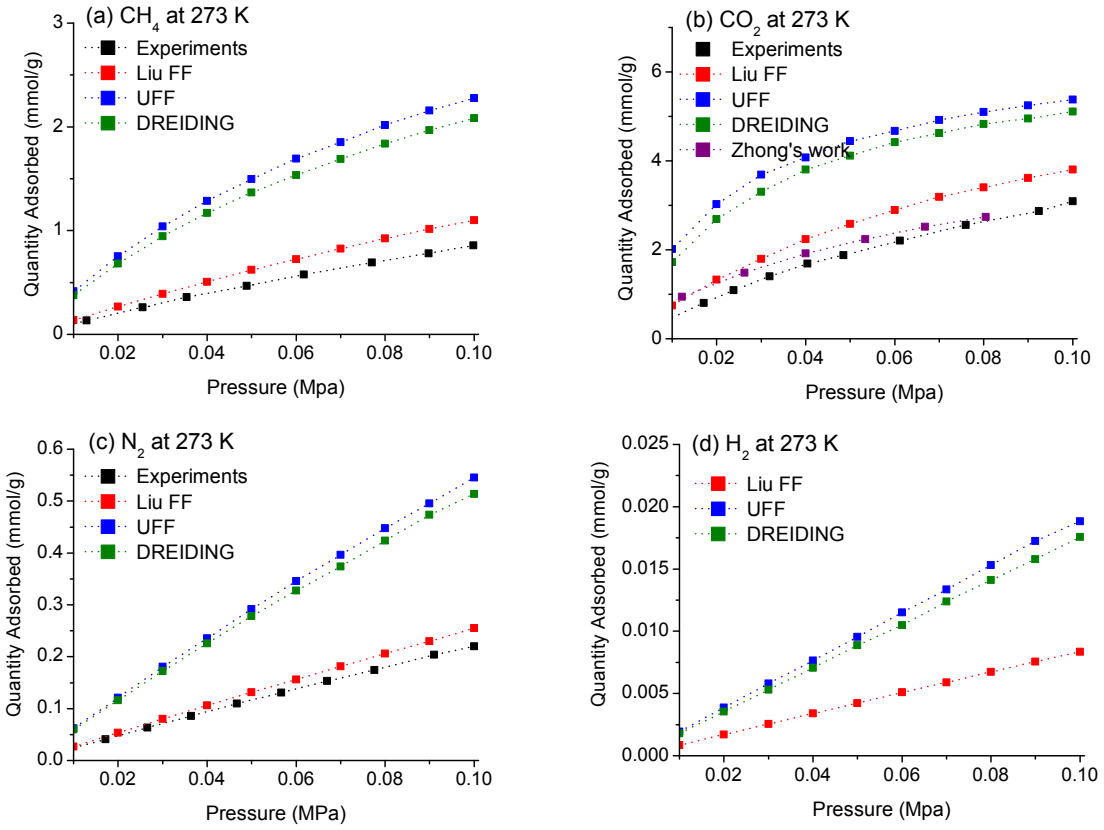

Figure 6.2. Comparison of experiments [34, 47] and molecular simulation results for single-component adsorption isotherms of (a)CH_4, (b)CO_2, (c)N_2, (d)H_2 at 273 K in ZIF-69. The CO_2 simulation results of Zhong's group [40] are also included in (b).

6.4. Effect of Force Fields on the Adsorbent Performance of ZIFs

Adsorption selectivity and working capacity are the two important factors that determine the efficiency of an adsorption-based separation process. One would expect to see both high adsorption selectivity and working capacity for the best adsorbent materials. Figure 6.3 represents the adsorption selectivity and working capacity of ZIF-68 and ZIF-69 for CH_4/H_2, CO_2/CH_4, CO_2/H_2 and CO_2/N_2 separations. In order to better evaluate the performance of ZIF adsorbents, the results are compared with the separation performances of zeolites and MOFs [19]. Figure 6.3(a) shows that both ZIF-68 and ZIF-69 are very promising candidates for CH_4/H_2 separation due to their higher CH_4 selectivities (20-40) than several zeolites and

MOFs. The CH_4 working capacity of ZIFs are similar to that of zeolites and MOFs, around 1.7-2.5 mol CH_4/kg adsorbent. Figure 6.3(b) suggests that ZIF-68 and ZIF-69 are also good adsorbents for CO_2/CH_4 separation. The CO_2 selectivities (~5) are higher than the selectivity of industrially important zeolites such as DDR. The CO_2 working capacities are around 3 mol CO_2/kg adsorbent similar to MOFs and zeolites. The CO_2/H_2 selectivities of ZIF adsorbents are high (>100) but the CO_2 working capacities are much lower than the other nanoporous adsorbents as shown in Figure 6.3(c). These low working capacities are related to the bulk composition of CO_2/H_2 mixture. As explained before, in order to perform the EMD simulations of CO_2/H_2 mixture in a statistically accurate manner, we set the bulk gas composition of the mixture to 1/99. Since the feed mixture is very dilute in CO_2, CO_2 working capacity of both ZIFs are estimated to be low compared to other nanoporous materials' working capacity which are calculated for CO_2/H_2:15/85 mixtures. Finally in CO_2/N_2 separations, ZIF-68 and ZIF-69 perform similar to zeolites with an adsorption selectivity of 20-40 as can be seen from Figure 6.3(d).

The highest adsorption selectivities are reported for CO_2/H_2 mixture whereas the lowest ones are reported for CO_2/CH_4 mixtures. This can be explained by the competition of gas molecules for adsorption sites in ZIFs. Since CO_2 (H_2) is the most (less) favorably adsorbed gas in ZIF-68 and ZIF-69 as shown in Figures 6.1 and 6.2, the highest adsorption selectivity is observed for CO_2/H_2 mixture. CH_4 is the second most preferred molecule for adsorption therefore there is a strong competition between CO_2 and CH_4 for the same adsorption sites, leading to lower CO_2 selectivities compared to other mixtures. Figure 6.3 suggests that separation performance of ZIF-69 is better than ZIF-68 for all mixtures which agrees with the experimental observations of Banerjee et al. [34] who calculated the selectivities from the ratio of slope of single-component gas adsorption isotherms. They reported CO_2/CH_4 selectivity of ZIF-68 and ZIF-69 as 5 and 5.5, respectively. These are consistent with the selectivities we calculated from mixture GCMC simulations using Liu FF (UFF), 4.0 (4.8) and 4.4 (5.5) for ZIF-68 and ZIF-69, respectively at 298 K, 1 bar. Experiments also predicted the CO_2/N_2 adsorption selectivity of ZIF-68 and ZIF-69 as 18.7 and 20 which also agree well with simulation results of 15.0 and 19.6 using Liu FF at 1 bar.

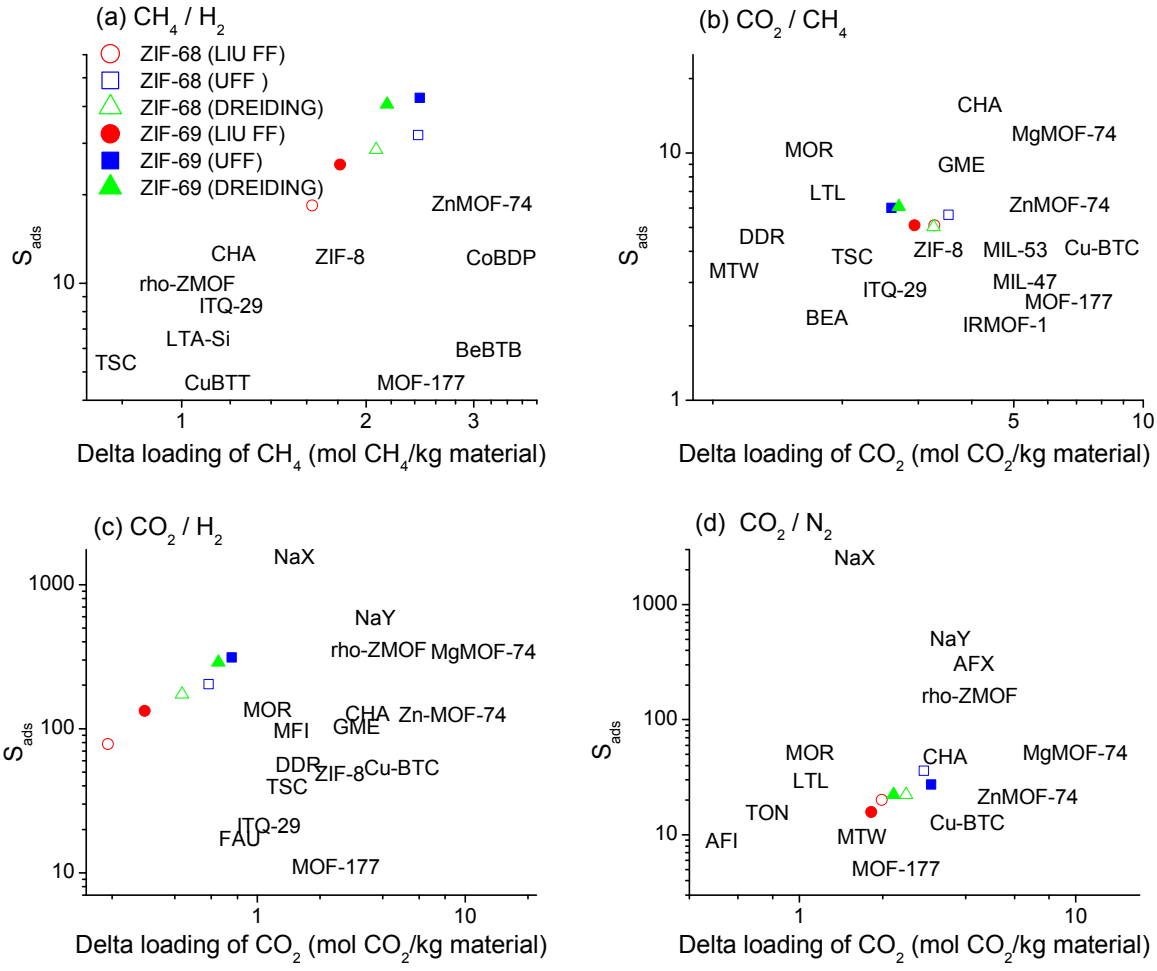

Figure 6.3. Adsorption-based separation performances of ZIF-68 and ZIF-69 for (a)CH_4/H_2, (b)CO_2/CH_4, (c)CO_2/H_2 and (d)CO_2/N_2 mixtures. The compositions of the bulk gas mixtures are (a)50/50, (b)50/50, (c)1/99 and (d)15/85, respectively. The adsorption and desorption pressures are 1 MPa and 0.1 MPa, respectively at 298 K. Data for other materials are shown for comparison and taken from Krishna et al. [19] in which compositions of CH_4/H_2, CO_2/CH_4, CO_2/H_2, and CO_2/N_2 are 50/50, 50/50, 15/85 and 15/85, respectively at 300 K.

Adsorption selectivities and working capacities of ZIFs are predicted using three different FFs in Figure 6.3. Figure 6.3(a) shows that CH_4 selectivities and working capacities predicted by UFF, DREIDING and Liu FF are all different from each other. UFF (Liu FF) gives the highest (lowest) selectivity and capacity predictions. For example, molecular simulations based on UFF predict a CH_4 selectivity (working capacity) of 31.9 (2.43 mol CH_4/kg ZIF) for ZIF-68 at 1 MPa and 298 K whereas simulations based on Liu FF predict a selectivity (working capacity) of 18.3 (1.63 mol CH_4/kg ZIF) for ZIF-68 under the same conditions. This result indicates that FF used in the simulations may have important effects on the quantitative

assessment of adsorbent's performance. Similarly in CO_2/H_2 separations, UFF gives the highest and Liu FF gives the lowest estimates for selectivity and capacity. Figure 6.3(c) shows that simulations based on UFF predict a CO_2/H_2 selectivity (working capacity) of 202 (0.58 mol CO_2/kg ZIF) for ZIF-68 at 1 MPa and 298 K whereas simulations based on Liu FF predict a selectivity (working capacity) of 77 (0.19 mol CO_2/kg ZIF) for ZIF-68 under the same conditions. It is important to note that adsorption of H_2 is very low in ZIFs and it does not change significantly based on the FF type whereas adsorption of the strongly adsorbed component (CH_4 in CH_4/H_2 mixture and CO_2 in CO_2/CH_4 mixture) is much more affected by the FF choice. Adsorption selectivity and working capacity predictions for CO_2/CH_4 and CO_2/N_2 mixtures did not significantly change when the FF is changed as can be seen from Figures 6.3(b) and 6.3(d). For example, Liu FF predicts the CO_2/CH_4 selectivity (working capacity) as 5.1 (3.27 mol CO_2/kg ZIF) for ZIF-68 whereas UFF estimates the selectivity (working capacity) as 5.6 (3.53 mol CO_2/kg ZIF).

In order to better evaluate the adsorption-based gas separation performances of ZIF-68 and ZIF-69, S_{sp} values and regenerability of these materials are computed for each gas separation of interest and listed these values in Tables B2 and B3 (See Appendix B). The S_{sp} predictions of three different FFs are close to each other for CO_2/CH_4 and CH_4/N_2 mixtures. The discrepancy between the S_{sp} values calculated from different FFs is obvious for CO_2/H_2 and CO_2/N_2 mixtures. In these mixtures, CO_2 is strongly adsorbed compared to weakly adsorbed H_2 and N_2 molecules therefore, adsorption selectivity is high. Since the S_{sp} formula includes square of the adsorption selectivity, S_{sp} estimates of different FFs vary significantly for these two mixtures. The S_{sp} values of ZIF-68 and ZIF-69 are also compared with other adsorbents. For example, Bae et al. [82] recently reported that HKUST-1 (CuBTC) is one of the best adsorbents with an S_{sp} value of 21 for separation of CO_2/CH_4:50/50 mixture at an adsorption pressure of 0.5 MPa and desorption pressure of 0.1 MPa. The S_{sp} values for ZIF-68 and ZIF-69 (30 and 49) calculated in this study are higher than the S_{sp} of HKUST-1. It is important to note that our S_{sp} values are calculated from mixture GCMC simulations where the competition effects between different gas species are taken into account whereas Bae's values are predicted from single-component adsorption data. Ozturk et al. [98] recently reported S_{sp} values for various porous coordination networks (PCNs) and best performing one, PCN-26, has a better performance (S_{sp} of 162) than ZIF-68 and ZIF-69 for CO_2/CH_4 mixture under the

same conditions. Erucar et al. [99] also reported the S_{sp} of Zn-Atz as 46.15 for CO_2/CH_4:50/50 mixture, which is close to the S_{sp} values of two ZIFs studied.

6.5. Effect of Force Fields on the Membrane Performance of ZIFs

Permeation selectivity and permeability are the two important factors that determine the efficiency of a membrane-based separation process. In order to compute them, diffusivities of gas mixtures in ZIFs' pores must be known. Figure 6.4 shows the self-diffusivities of each gas component in their binary mixtures calculated from EMD simulations using different FFs. There is not a significant change in the calculated diffusivities when FF is changed in EMD simulations. As expected from the sizes and weight of the molecules, H_2 is the fastest and CO_2 is the slowest molecule in the mixtures whereas the diffusivities of CH_4 and N_2 are close to each other.

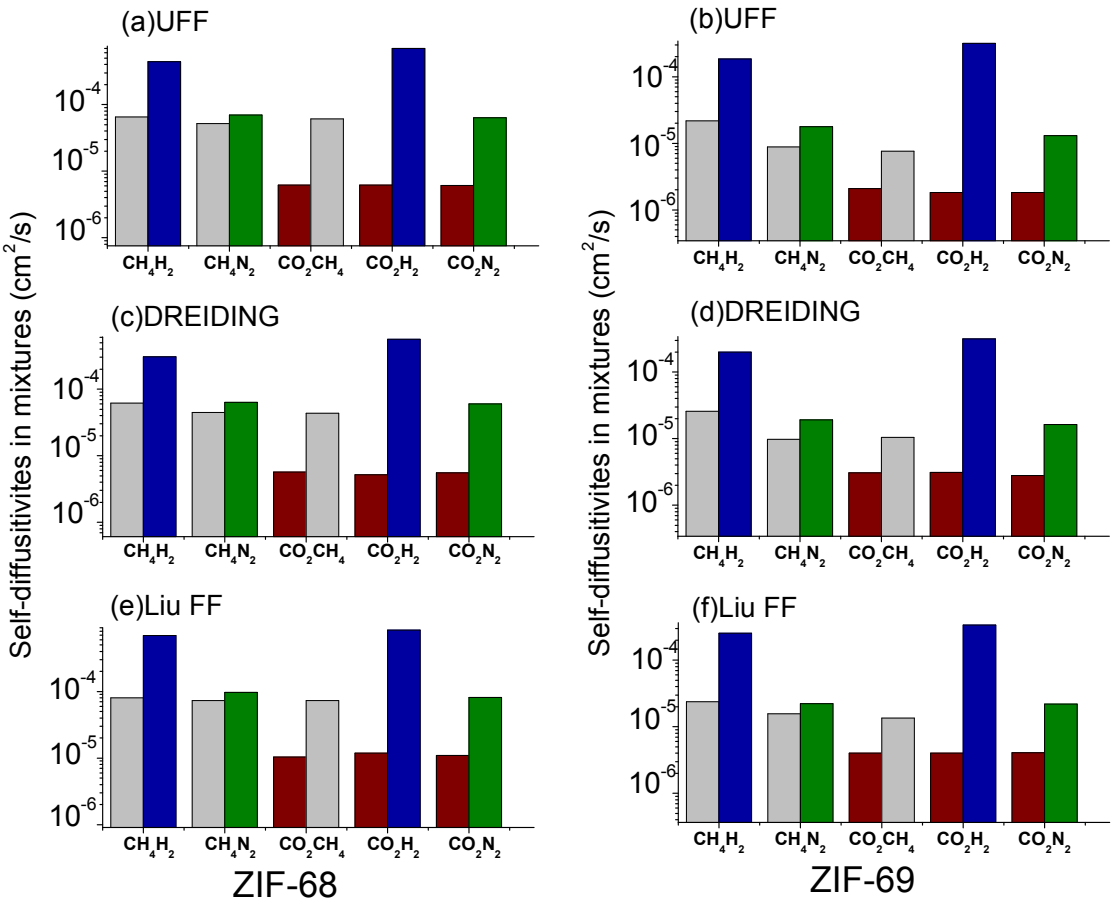

Figure 6.4. Self-diffusivities of each component in CH_4/H_2, CH_4/N_2, CO_2/CH_4, CO_2/H_2 and CO_2/N_2 mixtures in ZIF-68 and ZIF-69 at 298 K and 1 MPa. The compositions of the bulk gas mixtures are 50/50, 50/50, 50/50, 1/99 and 15/85, respectively.

Figure 6.5 compares the selectivity and permeability of ZIF-68 and ZIF-69 membranes calculated in this work with the separation performance of zeolites and MOFs taken from the literature [19]. Both high membrane selectivity and permeability are desired therefore, the best membrane candidates are supposed to be at the upper right region in the figure. Figure 6.5(a) shows that ZIF-68 and ZIF-69 are very promising membrane candidates for CH_4/H_2 separation due to their high CH_4 selectivities (2.1-5.7) in contrast to traditional zeolites LTA and CHA which are H_2 selective (CH_4 selectivity of 0.01-0.1) due to their narrow pore sizes that control the molecular diffusion. Since ZIF-68 and ZIF-69 have larger pore openings (4.78/8.89 Å and 7.21/9.97 Å), permeability of CH_4 (>2×104 Barrer) is also significantly larger in these ZIFs than that in ZIF-8, LTA, CHA (<0.1×104 Barrer).

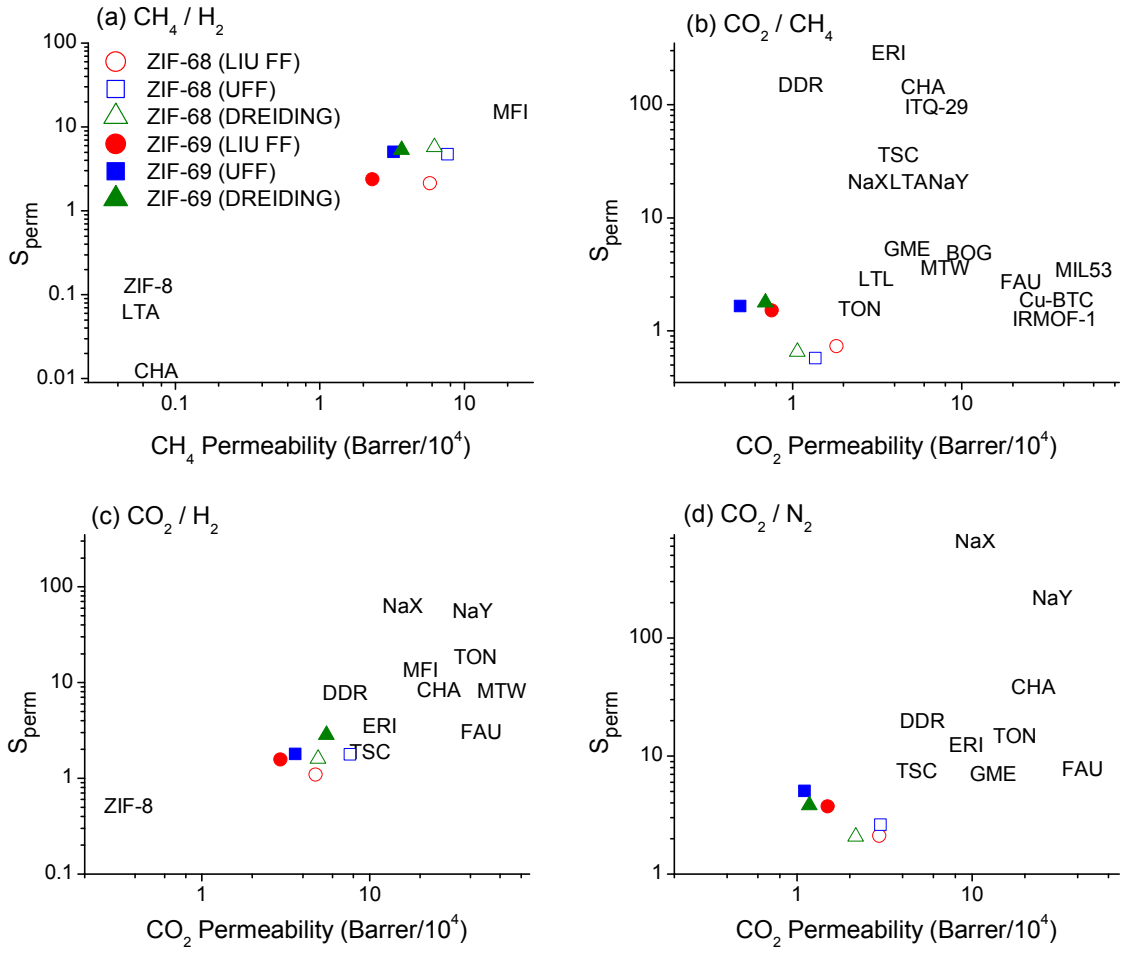

Figure 6.5. Membrane-based separation performances of ZIF-68 and ZIF-69 for (a)CH_4/H_2, (b)CO_2/CH_4, (c)CO_2/H_2 and (d)CO_2/N_2 mixtures. The compositions of the bulk gas mixtures are (a)50/50, (b)50/50, (c)1/99 and (d)15/85 at 298 K. The feed and permeate pressures are set to 1 MPa and vacuum, respectively at 298 K. Data for other materials is

shown for comparison and taken from Krishna et al. [19] in which compositions of CH_4/H_2, CO_2/CH_4, CO_2/H_2, and CO_2/N_2 as 50/50, 50/50, 15/85 and 15/85, respectively at 300 K.

Figure 6.5(b) shows that ZIF-68 and ZIF-69 are not highly promising materials for CO_2/CH_4 separation because of their low CO_2 selectivities. ZIF-69 is weakly CO_2 selective (1.5-1.8) whereas ZIF-68 is weakly CH_4 selective (1.4-1.75). This result can be explained by the low adsorption and diffusion selectivities of ZIFs toward CO_2. As discussed in the previous section, CO_2/CH_4 adsorption selectivity of ZIFs is already low (~5). The CO_2/CH_4 diffusion selectivity of ZIF-68 (ZIF-69) is around 0.1 (0.3) since CO_2 diffuses slowly compared to CH_4 in both materials' pores as shown in Figure 6.4. As a result, the permeation selectivities of ZIF membranes are very low. Figure 6.5(c) represents that CO_2/H_2 permeation selectivities of ZIF-68 and ZIF-69 are around 1.5-2.8, these values are close to zeolites ITQ-29 (1.8) and FAU (2.9). ZIF-68 and ZIF-69 exhibit high adsorption selectivity for CO_2 over H_2 (>100, see Figure 6.3(c)). However, the diffusion selectivity favors H_2 over CO_2 since light and weakly adsorbed H_2 molecules diffuses a lot faster than heavier and strongly adsorbed CO_2 molecules (see Figure 6.4). As a result high CO_2 adsorption selectivities are compensated by the low CO_2 diffusion selectivities, which is a very common observation for MOFs [81]. The same discussion is valid for CO_2/N_2 separation. As can be seen from Figure 6.5(d), the selectivity and permeability of ZIFs cannot exceed those of zeolites for this separation. Comparison of Figures 6.3 and 6.5 illustrates that ZIFs are more promising candidates to be used adsorbents rather than membranes for the gas separations studied since they offer higher selectivities as adsorbents.

The effect of FFs on the predicted membrane-based separation performances of ZIF-68 and ZIF-69 is also analyzed. Changing the FF does not make a significant difference on the estimated membrane performance of ZIFs. This can be explained by the individual contributions of adsorption and diffusion selectivities to the membrane selectivity. Generic FFs, UFF and DREIDING, tend to overestimate the adsorption selectivity compared to Liu FF. Since strongly adsorbed gas molecules move slowly compared to the weakly adsorbed ones, diffusion selectivity predictions of UFF and DREIDING are less than the predictions of Liu FF. For example, adsorption selectivity of ZIF-68 for CO_2/H_2 mixtures is calculated as 77.8 by Liu FF, 173 by DREIDING and 203 by UFF. The diffusion selectivities of ZIF-68 for the same mixture are calculated as 0.014 by Liu FF, 0.009 by DREIDING and 0.008 by UFF. As a result, the permeation selectivity of ZIF-68 estimated from different FFs become similar to each other (1.1 by Liu FF, 1.6 by DREIDING and 1.8 by UFF). An important result that is

extracted from Figure 6.5 is that using different FFs does not have a very significant effect on the predicted permeation selectivity of ZIF-68 and ZIF-69. The predictions of Liu FF, which is specifically developed to match the simulation results with the experiments for gas adsorption isotherms, give similar membrane selectivity estimates with the generic FFs, UFF and DREIDING.

In order to better understand which FF makes the best predictions for gas permeability, a comparison between experiments and simulations must be done. A thin film ZIF-69 membrane has been recently fabricated and tested for gas permeance (permeability normalized by the thickness of the membrane) [25, 100, 101]. The simulation results are compared with the experimental gas permeance data of CO_2/N_2 and CO_2/CH_4 mixtures through ZIF-69 membrane under the same conditions and showed the results in Figure 6.6. There is a reasonable agreement between our simulations and experimental measurement for N_2 and CH_4 permeance when Liu FF or DREIDING is used in simulations. The predictions of UFF-based simulations slightly overestimated the experimental results but still in a reasonable agreement. The CO_2 permeance of CO_2/N_2 mixture is estimated accurately by the three FFs whereas CO_2 permeance of CO_2/CH_4 mixture is slightly overestimated. In a previous simulation study, Atci et al. [53] underestimated the experimental permeance results using UFF whereas a better agreement with the experiments is found in this work. The main difference between Atci's work and this work is the different potential models used for gas molecules and different partial charge assignment method applied to ZIFs as can be seen from Table B1 in Appendix B. To summarize, Figure 6.6 suggests that generic FFs such as UFF and DREIDING can be used to make initial estimates for the gas permeability of new membrane materials.

Almost all of the molecular simulations for ZIFs in the literature used rigid framework assumption because it saves a significant amount of computational time and molecular simulations should be performed for multiple materials on time scales shorter than the same materials can be assessed experimentally. Since adsorption involves low energy equilibrium configurations, the flexibility of the framework has a marginal effect on the adsorption of gas molecules [47]. On the other hand, flexibility may be an important issue for diffusion of large gas molecules in the materials having narrow pore windows [93]. Molecular simulations that do not consider framework flexibility can overestimate the selectivity of the membranes since they assume that the gas species larger than the material's pore size cannot permeate through

the membrane. The good agreement between our calculated gas permeances of ZIF-69 membranes from simulations assuming rigid framework and experiments confirms the reliability of our assumption. It is important to note that the idea of our calculations is that once the potential value of a material has been demonstrated using molecular simulations, a more detailed calculation approach including framework flexibility can be used to increase the precision of the assessment.

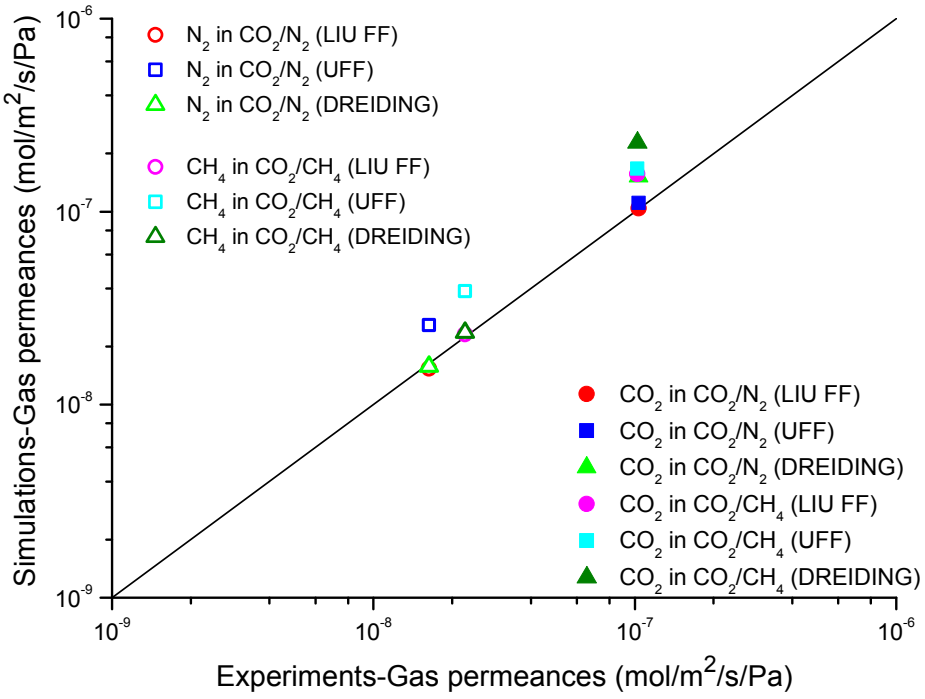

Figure 6.6. Comparison of simulations with the experimental data [25] for permeation of equimolar binary gas mixtures through ZIF-69 membrane at 298 K and 0.1 MPa.

Chapter 7: Conclusion

In this thesis, adsorption-based and membrane-based separation performances of ZIFs for CH_4/H_2, CH_4/N_2, CO_2/CH_4, CO_2/H_2 and CO_2/N_2 mixtures are evaluated using atomically detailed simulations. The main goal in this study is to screen ZIFs as adsorbents and membranes for gas separation applications using time efficient single-component molecular simulations and compare the results with the mixture simulations to understand if ideal selectivity is different than the mixture diffusivity. Results suggest that if there is no information on mixture adsorption and/or diffusion of gases in ZIFs, intrinsic selectivity calculated from single-component adsorption and diffusion data can be efficiently used to make initial predictions about the separation performance of ZIFs. However, ideal and mixture selectivity are found to be very different if (a) one of the gas components is strongly favored over another, e.g. CO_2/H_2 adsorption in ZIFs which have functional groups that make strong electrostatic interactions with CO_2, (b) mixture effects are dominant and gas species change the diffusion rate of each other. Therefore, if a material is identified to show high performance in CO_2 separations based on intrinsic selectivity, it would be useful to study this material in more detail by considering mixture adsorption and diffusion. The single-component and mixture data-based screening approach introduced here can be used to predict the selectivity of a large variety of ZIFs including the hypothetical ones in adsorption and membrane-based gas separation applications.

ZIF-78 and ZIF-79 are the best candidates for adsorption based separation for all CO_2/CH_4, CO_2/N_2, CO_2/H_2 and CH_4/H_2 mixtures. However, adsorption selectivity is not the only criteria to evaluate the performance of a material. When permeation selectivities are considered ZIF-11 and ZIF-12 are more promising than other ZIFs for CO_2/CH_4, CO_2/N_2, CO_2/H_2 mixtures. This result provides the idea that ZIF-11 and ZIF-12 are the best candidates

in membrane-based separation of CO_2 mixtures. On the other hand, ZIF-2 and ZIF-79 have the best membrane performance for CH_4/H_2 separation.

ZIFs are assumed as rigid structure in the simulations of this thesis. On the other hand, experiments and simulation studies show that flexibility may become an important issue for adsorption and diffusion of large gas molecules in the narrow pore windows of ZIF-8 [62]. For example, the unexpected adsorption of large molecules on ZIF-8 suggests the existence of structural flexibility [102, 103]. Molecular simulations that do not consider framework flexibility can overestimate the selectivity of the membranes since they assume that the gas species larger than the pore size of the material cannot permeate through the membrane. Using DFT (Density Functional Theory) calculations for this type of materials will be appropriate to evaluate the performance of the material, especially for diffusion characteristics [104]. Furthermore, the good agreement between calculated gas permeances of ZIF membranes using rigid frameworks [53] and experiments confirms the reliability of this assumption. It is important to note that the idea of these calculations is that once the potential value of a material has been demonstrated using molecular simulations, a more detailed calculation approach including framework flexibility can be used to increase the precision of the assessment.

Secondly, the effect of force field (FF) parameters used in molecular simulations is examined on the predicted gas separation performance of ZIF adsorbents and membranes. For this investigation, adsorption and permeation-based separation performances of ZIF-68 and ZIF-69 for CH_4/H_2, CH_4/N_2, CO_2/CH_4, CO_2/H_2 and CO_2/N_2 mixtures are calculated using molecular simulations with three different FFs. Two of the FFs are generic, UFF and DREIDING and the other is a tailored one, Liu FF, designed to match the simulation results with the experimental single-component adsorption isotherms. Results show that predictions of molecular simulation for adsorption selectivities are sensitive to FF type. Generic FFs generally tend to overestimate the gas adsorption capacities hence adsorption selectivities of ZIF-68 and ZIF-69 compared to Liu FF. However, the difference between predicted adsorption selectivities is not extremely high to change the conclusion about the separation performance of the material. The quantitative accuracy of the molecular simulations must allow making confident judgments for identifying the promising and unpromising materials and all three FFs are able to identify the promising adsorbent materials that exhibit high adsorption selectivity.

The results show that membrane selectivities predicted by different FFs are very similar to each other since overestimation of adsorption selectivities and underestimations of diffusion selectivities by generic FFs balance each other. This result suggests that a generic FF can be safely used to make an initial prediction for a candidate membrane material without developing a material-specific FF. This is an important result for screening of new materials because experimental data is generally not available for the newly synthesized materials and describing a tailored FF based on experiments is not possible for the new materials. Furthermore, it is important to note that fitting of FF parameters to match the simulation results with the experiments may not be always a good strategy since the experimental gas uptake capacities of ZIFs mostly depend on the method of pretreatment of ZIFs.

Comparison of separation performance of ZIF-68 and ZIF-69 with traditional zeolites and MOFs show that ZIFs can be promising adsorbent materials for CH_4/H_2, CH_4/N_2, CO_2/CH_4, CO_2/H_2 separations and promising membrane materials for CH_4/H_2 and CO_2/H_2 separations. It is better to use ZIFs as adsorbents rather than membranes since they offer higher adsorption selectivity than permeation selectivity for the gas mixtures studied.

BIBLIOGRAPHY

[1] Yang, H., et al., *Progress in Carbon Dioxide Separation and Capture: A Review.* Journal of Environmental Sciences, 2008. **20**(1): p. 14-27.

[2] Bernardo, P., Drioli, E. and Golemme, G., *Membrane Gas Separation: A Review/State of the Art.* Industrial & Engineering Chemistry Research, 2009. **48**(10): p. 4638-4663.

[3] Geankoplis, C.J., *Transport Processes and Unit Operations.* 1993.

[4] Reay, D., Ramshaw, C. and Harvey, A., *Process Intensification: Engineering for Efficiency, Sustainability and Flexibility*. 2013: Butterworth-Heinemann Press.

[5] Takht R. M., Kaghazchi, T. and Kargari, A., *Application of Membrane Separation Processes in Petrochemical Industry: A Rreview.* Desalination, 2009. **235**(1–3): p. 199-244.

[6] Bekkum, H., Flanigen, E. and Jansen, J., *Introduction to Zeolite Science and Practice.* Stud. Surf. Sci. Catal, 1991. **58**: p. 201.

[7] Auerbach, S.M., Carrado, K.A. and Dutta, P.K., *Handbook of Zeolite Science and technology*. 2003: CRC Press.

[8] Isaeva, V.I. and Kustov, L.M., *Metal-Organic Frameworks-New Materials for Hydrogen Storage.* Russian Journal of General Chemistry, 2007. **77**(4): p. 721-739.

[9] Mueller, U., et al., *Metal-Organic Frameworks-Prospective Industrial Applications.* Journal of Materials Chemistry, 2006. **16**(7): p. 626-636.

[10] Sattler, K.D., *Handbook of Nanophysics: Principles and Methods*. 2010: CRC Press.

[11] Hayashi, H., et al., *Zeolite A Imidazolate Frameworks.* Nature materials, 2007. **6**(7): p. 501-506.

[12] Wang, B., et al., *Colossal Cages in Zeolitic Imidazolate Frameworks as Selective Carbon Dioxide Reservoirs.* Nature, 2008. **453**(7192): p. 207-211.

[13] Phan, A., et al., *Synthesis, Structure, and Carbon Dioxide Capture Properties of Zeolitic Imidazolate Frameworks.* Acc. Chem. Res, 2010. **43**(1): p. 58-67.

[14] Pérez-Pellitero, J., et al., *Adsorption of CO_2, CH_4, and N_2 on Zeolitic Imidazolate Frameworks: Experiments and Simulations.* Chemistry-A European Journal, 2010. **16**(5): p. 1560-1571.

[15] Koros, W.J. and Mahajan, R., *Pushing the Limits on Possibilities for Large Scale Gas Separation: Which Strategies?* Journal of Membrane Science, 2000. **175**(2): p. 181-196.

[16] Budd, P.M., et al., *Gas Separation Membranes from Polymers of Intrinsic Microporosity.* Journal of Membrane Science, 2005. **251**(1–2): p. 263-269.

[17] Robeson, L.M., *Correlation of Separation Factor versus Permeability for Polymeric Membranes.* Journal of Membrane Science, 1991. **62**(2): p. 165-185.

[18] Robeson L.M., *The Upper Bound Revisited.* Journal Membrane Science, 2008. **320**: p. 1-2.

[19] Krishna, R. and van Baten, J.M., *In Silico Screening of Metal-Organic Frameworks in Separation Applications.* Physical Chemistry Chemical Physics, 2011. **13**(22): p. 10593-10616.

[20] Li, L., et al., *Infiltration of Precursors into a Porous Alumina Support for ZIF-8 Membrane Synthesis.* Microporous and Mesoporous Materials, 2013. **168**(0): p. 15-18.

[21] Li, Y., et al., *Zeolitic Imidazolate Framework ZIF-7 Based Molecular Sieve Membrane for Hydrogen Separation.* Journal of Membrane Science, 2010. **354**(1–2): p. 48-54.

[22] Huang, A., et al., *Molecular-Sieve Membrane with Hydrogen Permselectivity: ZIF-22 in LTA Topology Prepared with 3-Aminopropyltriethoxysilane as Covalent Linker.* Angewandte Chemie, 2010. **122**(29): p. 5078-5081.

[23] Huang, A., Dou, W. and Caro, J.R., *Steam-Stable Zeolitic Imidazolate Framework ZIF-90 Membrane with Hydrogen Selectivity through Covalent Functionalization.* Journal of the American Chemical Society, 2010. **132**(44): p. 15562-15564.

[24] Bux, H., et al., *Zeolitic Imidazolate Framework Membrane with Molecular Sieving Properties by Microwave-assisted Solvothermal Synthesis.* Journal of the American Chemical Society, 2009. **131**(44): p. 16000-16001.

[25] Liu, Y., et al., *Synthesis and Characterization of ZIF-69 Membranes and Separation for CO_2/CO Mixture.* Journal of Membrane Science, 2010. **353**(1): p. 36-40.

[26] Mellot-Draznieks, C. and Kerkeni, B., *Exploring the Interplay between Ligand and Topology in Zeolitic Imidazolate Frameworks with Computational Chemistry.* Molecular Simulation, 2014. **40**(1-3): p. 25-32.

[27] Lai, L.S., et al., *Zeolite Imidazole Frameworks Membranes for CO_2/CH_4 Separation from Natural Gas: A Review.* Journal of Applied Sciences, 2014. **14**(11).

[28] Huang, L., et al., *Carbon Dioxide Selective Adsorption within a Highly Stable Mixed-Ligand Zeolitic Imidazolate Framework.* Inorganic Chemistry Communications, 2014. **46**: p. 9-12.

[29] Park, K.S., et al., *Exceptional Chemical and Thermal Stability of Zeolitic Imidazolate Frameworks.* Proceedings of the National Academy of Sciences, 2006. **103**(27): p. 10186-10191.

[30] Banerjee, R., et al., *High-Throughput Synthesis of Zeolitic Imidazolate Frameworks and Application to CO_2 Capture.* Science, 2008. **319**(5865): p. 939-943.

[31] Ravichandar, B., *Computational Study of Adsorption and Diffusion in Metal-Organic Frameworks.* 2009.

[32] Morris, W., et al., *Crystals as Molecules: Postsynthesis Covalent Functionalization of Zeolitic Imidazolate Frameworks.* Journal of the American Chemical Society, 2008. **130**(38): p. 12626-12627.

[33] Morris, W., et al., *A Combined Experimental-Computational Study on the Effect of Topology on Carbon Dioxide Adsorption in Zeolitic Imidazolate Frameworks.* The Journal of Physical Chemistry C, 2012. **116**(45): p. 24084-24090.

[34] Banerjee, R., et al., *Control of Pore Size and Functionality in Isoreticular Zeolitic Imidazolate Frameworks and Their Carbon Dioxide Selective Capture Properties.* Journal of the American Chemical Society, 2009. **131**(11): p. 3875-3877.

[35] Li, Y.S., et al., *Molecular Sieve Membrane: Supported Metal–Organic Framework with High Hydrogen Selectivity.* Angewandte Chemie, 2010. **122**(3): p. 558-561.

[36] Dong, X., et al., *Synthesis of Zeolitic Imidazolate Framework-78 Molecular-Sieve Membrane: Defect Formation and Elimination.* Journal of Materials Chemistry, 2012. **22**(36): p. 19222-19227.

[37] Han, S.S., Choi S.H. and Goddard W.A., *Zeolitic Imidazolate Frameworks as H_2 Adsorbents: Ab Initio Based Grand Canonical Monte Carlo Simulation.* The Journal of Physical Chemistry C, 2010. **114**(27): p. 12039-12047.

[38] Chen, E.Y., et al., *Effects of Substituent Groups and Central Metal Ion on Hydrogen Adsorption in Zeolitic Imidazolate Frameworks.* Chemical Engineering Science, 2013. **97**: p. 60-66.

[39] Liu, B. and Smit, B., *Molecular Simulation Studies of Separation of CO_2/N_2, CO_2/CH_4, and CH_4/N_2 by ZIFs.* The Journal of Physical Chemistry C, 2010. **114**(18): p. 8515-8522.

[40] Liu, D., et al., *Understanding the Adsorption and Diffusion of Carbon Dioxide in Zeolitic Imidazolate Frameworks: A Molecular Simulation Study.* The Journal of Physical Chemistry C, 2009. **113**(12): p. 5004-5009.

[41] Rankin, R.B., et al., *Adsorption and Diffusion of Light Gases in ZIF-68 and ZIF-70: A Simulation Study.* J. Phys. Chem. C 2009. **113**: p. 16906–16914.

[42] Krishna, R. and van Baten, J.M., *In Silico Screening of Zeolite Membranes for CO_2 Capture.* J. Memb. Sci., 2010. **360**: p. 323-333.

[43] Keskin, S., *Atomistic Simulations for Adsorption, Diffusion, and Separation of Gas Mixtures in Zeolite Imidazolate Frameworks.* J. Phys. Chem. C, 2011. **115**(3): p. 800-807.

[44] Liu, J., et al., *Molecular Simulations and Theoretical Predictions for Adsorption and Diffusion of CH_4/H_2 and CO_2/CH_4 Mixtures in ZIF-68 and ZIF-70.* J. Phys. Chem. C, 2011. **115**(25): p. 12560-12566.

[45] Wu, D., et al., *Large-Scale Computational Screening of Metal-Organic Frameworks for CH_4/H_2 Separation.* AIChE Journal, 2011: p. 58, 2078-2074.

[46] Huang, H., et al., *Effect of Temperature on Gas Adsorption and Separation in ZIF-8: A Combined Experimental and Molecular Simulation Study.* Chemical Engineering Science, 2011. **66**(23): p. 6297-6305.

[47] Babarao, R., Dai, S. and Jiang, D.E., *Effect of Pore Topology and Accessibility on Gas Adsorption Capacity in Zeolitic-Imidazolate Frameworks: Bringing Molecular Simulation Close to Experiment.* The Journal of Physical Chemistry C, 2011. **115**(16): p. 8126-8135.

[48] Sirjoosingh, A., Alavi, S. and Woo, T.K., *Grand-Canonical Monte Carlo and Molecular-Dynamics Simulations of Carbon-Dioxide and Carbon-Monoxide Adsorption in Zeolitic Imidazolate Framework Materials.* The Journal of Physical Chemistry C, 2010. **114**(5): p. 2171-2178.

[49] Hou, X.J. and Li, H., *Unraveling the High Uptake and Selectivity of CO_2 in the Zeolitic Imidazolate Frameworks ZIF-68 and ZIF-69.* The Journal of Physical Chemistry C, 2010. **114**(32): p. 13501-13508.

[50] Prakash, M., Sakhavand, N. and Shahsavari, R., *H_2, N_2, and CH_4 Gas Adsorption in Zeolitic Imidazolate Framework-95 and -100: Ab-Initio Based Grand Canonical Monte Carlo Simulations.* The Journal of Physical Chemistry C, 2013. **117**(46): p. 24407-24416.

[51] Li, B., Wei, S. and Chen, L., *Molecular simulation of CO_2, N_2 and CH_4 adsorption and separation in ZIF-78 and ZIF-79.* Molecular Simulation, 2011. **37**(13): p. 1131-1142.

[52] Rankin, R.B., et al., *Adsorption and Diffusion of Light Gases in ZIF-68 and ZIF-70: A Simulation Study.* The Journal of Physical Chemistry C, 2009. **113**(39): p. 16906-16914.

[53] Atci, E. and Keskin, S., *Understanding the Potential of Zeolite Imidazolate Framework Membranes in Gas Separations using Atomically Detailed Calculations.* The Journal of Physical Chemistry C, 2012. **116**(29): p. 15525-15537.

[54] Frenkel, D. and Smit, B., *Understanding Molecular Simulation: from Algorithms to Applications*. Vol. 1. 2001: Academic press.

[55] Morris, W., et al., *A Combined Experimental-Computational Investigation of Carbon Dioxide Capture in a Series of Isoreticular Zeolitic Imidazolate Frameworks.* Journal of the American Chemical Society, 2010. **132**(32): p. 11006-11008.

[56] Amrouche, H., et al., *Experimental and Computational Study of Functionality Impact on Sodalite-Zeolitic Imidazolate Frameworks for CO_2 Separation.* The Journal of Physical Chemistry C, 2011. **115**(33): p. 16425-16432.

[57] Kardar, M., *Statistical Physics of Particles*. 2007: Cambridge University Press.

[58] Atkins, P.W. and Paula, J.D., *The Elements of Physical Chemistry*. 2005: Oxford University Press New York, NY, USA:.

[59] Einstein, A., *Investigations on the Theory of the Brownian Movement*. 1956: Courier Dover Publications.

[60] Kärger, J., Ruthven, D.M. and Theodorou, D.N., *Diffusion in Nanoporous Materials*. 2012: John Wiley & Sons.

[61] Bezus, A.G., et al., *Molecular Statistical Calculation of the Thermodynamic Adsorption Characteristics of Zeolites using the Atom–Atom Approximation. Part 1. Adsorption of Methane by Zeolite NaX*. Journal of the Chemical Society, Faraday Transactions 2: Molecular and Chemical Physics, 1978. **74**: p. 367-379.

[62] Fairen-Jimenez, D., et al., *Opening the Gate: Framework Flexibility in ZIF-8 Explored by Experiments and Simulations.* Journal of the American Chemical Society, 2011. **133**(23): p. 8900-8902.

[63] Zheng, B., et al., *Force Field for Molecular Dynamics Computations in Flexible ZIF-8 Framework.* The Journal of Physical Chemistry C, 2012. **116**(1): p. 933-938.

[64] Coudert, F.X., et al., *Thermodynamic Methods and Models to Study Flexible Metal-Organic Frameworks.* Chem. Phys. Chem., 2011. **12**(2): p. 247-258.

[65] Hu, Z., Zhang, L. and Jiang, J., *Development of a Force Field for Zeolitic Imidazolate Framework-8 with Structural Flexibility.* The Journal of chemical physics, 2012. **136**(24): p. 244703.

[66] Smit, B. and Maesen, T.L., *Molecular Simulations of Zeolites: Adsorption, Diffusion, and Shape Selectivity.* Chemical reviews, 2008. **108**(10): p. 4125-4184.

[67] Griffiths, D.J., *Introduction to Quantum Mechanics*. 2005: Pearson Education India.

[68] Israelachvili, J.N., *Intermolecular and Surface Forces: Revised Third Edition*. 2011: Academic press.

[69] Dubbeldam, D., et al., *United Atom Force Field for Alkanes in Nanoporous Materials.* The Journal of Physical Chemistry B, 2004. **108**(33): p. 12301-12313.

[70] Pascual, P., et al., *Development of a Transferable Guest–Host Force Field for Adsorption of Hydrocarbons in Zeolites I. Reinvestigation of Alkane Adsorption in Silicalite by Grand Canonical Monte Carlo Simulation.* Physical Chemistry Chemical Physics, 2003. **5**(17): p. 3684-3693.

[71] Rappé, A.K., et al., *UFF, A Full Periodic Table Force Field for Molecular Mechanics and Molecular Dynamics Simulations.* Journal of the American Chemical Society, 1992. **114**(25): p. 10024-10035.

[72] Mayo, S.L., Olafson, B.D. and Goddard, W.A., *DREIDING: A Generic Force Field for Molecular Simulations.* Journal of Physical Chemistry, 1990. **94**(26): p. 8897-8909.

[73] Atci, E. and Keskin, S., *Atomically Detailed Models for Transport of Gas Mixtures in ZIF Membranes and ZIF/Polymer Composite Membranes.* Industrial & Engineering Chemistry Research, 2012. **51**(7): p. 3091-3100.

[74] Buch, V., *Path Integral Simulations of Mixed para-D_2 and ortho-D_2 Clusters: The Orientational Effects.* The Journal of chemical physics, 1994. **100**(10): p. 7610-7629.

[75] Martin, M.G. and Siepmann, J.I., *Transferable Potentials for Phase Equilibria. 1. United-Atom Description of n-alkanes.* The Journal of Physical Chemistry B, 1998. **102**(14): p. 2569-2577.

[76] Potoff, J.J. and Siepmann, J.I., *Vapor–Liquid Equilibria of Mixtures Containing Alkanes, Carbon Dioxide, and Nitrogen.* AIChE journal, 2001. **47**(7): p. 1676-1682.

[77] Makrodimitris, K., Papadopoulos, G.K. and Theodorou, D.N., *Prediction of Permeation Properties of CO_2 and N_2 through Silicalite via Molecular Simulations.* The Journal of Physical Chemistry B, 2001. **105**(4): p. 777-788.

[78] Xu, Q. and Zhong, C., *A General Approach for Estimating Framework Charges in Metal−Organic Frameworks.* The Journal of Physical Chemistry C, 2010. **114**(11): p. 5035-5042.

[79] Watanabe, T., Manz T.A., and Sholl D.S, *Accurate Treatment of Electrostatics During Molecular Adsorption in Nanoporous Crystals without Assigning Point Charges to Framework Atoms.* The Journal of Physical Chemistry C, 2011. **115**(11): p. 4824-4836.

[80] Hirotani, A., et al., *Grand Canonical Monte Carlo Simulation of the Adsorption of CO_2 on Silicalite and NaZSM-5.* Applied surface science, 1997. **120**(1): p. 81-84.

[81] Keskin, S. and Sholl, D.S., *Efficient Methods for Screening of Metal Organic Framework Membranes for Gas Separations Using Atomically Detailed Models.* Langmuir, 2009. **25**(19): p. 11786-11795.

[82] Bae, Y.S. and Snurr, R.Q., *Development and Evaluation of Porous Materials for Carbon Dioxide Separation and Capture.* Angewandte Chemie International Edition, 2011. **50**(49): p. 11586-11596.

[83] Atci, E. and Keskin S., *Understanding the Potential of Zeolite Imidazolate Framework Membranes in Gas Separations Using Atomically Detailed Calculations.* Journal of Physical Chemistry C, 2012. **116**(29): p. 15525-15537.

[84] Park, K.S., et al., *Exceptional Chemical and Thermal Stability of Zeolitic Imidazolate Frameworks.* Proceedings of the National Academy of Sciences of the United States of America, 2006. **103**(27): p. 10186-10191.

[85] Yilmaz, G. and Keskin, S., *Predicting the Performance of Zeolite Imidazolate Framework/Polymer Mixed Matrix Membranes for CO_2, CH_4, and H_2 Separations*

Using Molecular Simulations. Industrial & Engineering Chemistry Research, 2012. **51**(43): p. 14218-14228.

[86] Ackerman, D.M., et al., *Diffusivities of Ar and Ne in Carbon Nanotubes.* Molecular Simulation, 2003. **29**(10-11): p. 677-684.

[87] Sanborn, M.J. and Snurr, R.Q., *Diffusion of Binary Mixtures of CF_4 and n-alkanes in Faujasite.* Separation and Purification Technology, 2000. **20**(1): p. 1-13.

[88] Skoulidas, A.I. and Sholl, D.S., *Self-Diffusion and Transport Diffusion of Light Gases in Metal-Organic Framework Materials Assessed Using Molecular Dynamics Simulations.* The Journal of Physical Chemistry B, 2005. **109**(33): p. 15760-15768.

[89] McEwen, J., Hayman, J.D. and Yazaydin, A.O., *A Comparative Study of CO_2, CH_4 and N_2 Adsorption in ZIF-8, Zeolite-13X and BPL Activated Carbon.* Chemical Physics, 2013. **412**(0): p. 72-76.

[90] Qian, J., Sun, F. and Qin, L. *Hydrothermal Synthesis of Zeolitic Imidazolate Framework-67 (ZIF-67) Nanocrystals.* Materials Letters, 2012. **82**(0): p. 220-223.

[91] Sholl, D.S., *Understanding Macroscopic Diffusion of Adsorbed Molecules in Crystalline Nanoporous Materials via Atomistic Simulations.* Acc. Chem. Res., 2006. **39**(6): p. 403-411.

[92] Amrouche, H., et al., *Experimental and Computational Study of Functionality Impact on Sodalite-Zeolitic Imidazolate Frameworks for CO_2 Separation.* The Journal of Physical Chemistry C, 2011. **115**(33): p. 16425-16432.

[93] Hertäg, L., et al., *Diffusion of CH_4 and H_2 in ZIF-8.* Journal of Membrane Science, 2011. **377**(1–2): p. 36-41.

[94] Pantatosaki, E., et al., *Probing the Hydrogen Equilibrium and Kinetics in Zeolite Imidazolate Frameworks via Molecular Dynamics and Quasi-Elastic Neutron Scattering Experiments.* The Journal of Chemical Physics, 2013. **138**(3): p. -.

[95] Parkes, M.V., et al., *Screening Metal-organic Frameworks for Selective Noble Gas Adsorption in Air: Effect of Pore Size and Framework Topology.* Physical Chemistry Chemical Physics, 2013. **15**(23): p. 9093-9106.

[96] Keskin, S., *Adsorption, Diffusion, and Separation of CH_4/H_2 Mixtures in Covalent Organic Frameworks: Molecular Simulations and Theoretical Predictions.* The Journal of Physical Chemistry C, 2011. **116**(2): p. 1772-1779.

[97] Atci, E., Erucar, I. and Keskin, S., *Adsorption and Transport of CH_4, CO_2, H_2 Mixtures in a Bio-MOF Material from Molecular Simulations.* The Journal of Physical Chemistry C, 2011. **115**(14): p. 6833-6840.

[98] Ozturk, T.N. and Keskin S., *Predicting Gas Separation Performances of Porous Coordination Networks Using Atomistic Simulations.* Industrial & Engineering Chemistry Research, 2013. **52**(49): p. 17627-17639.

[99] Erucar, I. and Keskin, S., *High CO_2 Selectivity of an Amine-Functionalized Metal Organic Framework in Adsorption-Based and Membrane-Based Gas Separations.* Industrial & Engineering Chemistry Research, 2013. **52**(9): p. 3462-3472.

[100] Liu, Y., et al., *Synthesis and Characterization of ZIF-69 Membranes and Separation for CO_2/CO Mixture.* Journal of Membrane Science, 2010. **353**(1–2): p. 36-40.

[101] Tzialla, O., et al., *Zeolite Imidazolate Framework–Ionic Liquid Hybrid Membranes for Highly Selective CO_2 Separation.* The Journal of Physical Chemistry C, 2013. **117**(36): p. 18434-18440.

[102] Moggach, S.A., Bennett, T.D. and Cheetham, A.K., *The Effect of Pressure on ZIF-8: Increasing Pore Size with Pressure and the Formation of a High-Pressure Phase at 1.47 GPa.* Angewandte Chemie, 2009. **121**(38): p. 7221-7223.

[103] Ania, C.O., et al., *Understanding Gas-Induced Structural Deformation of ZIF-8.* The Journal of Physical Chemistry Letters, 2012. **3**(9): p. 1159-1164.

[104] Watanabe, T., et al., *Computational Identification of a Metal Organic Framework for High Selectivity Membrane-based CO_2/CH_4 Separations: Cu(hfipbb)(H_2hfipbb)$_{0.5}$.* Physical Chemistry Chemical Physics, 2009. **11**(48): p. 11389-11394.

[105] Accelrys, I., *Material Studio, 3.0 V.* Accelrys Inc., San Diego,CA, 2003.

[106] Breneman, C.M. and Wiberg K.B., *Determining Atom-Centered Monopoles from Molecular Electrostatic Potentials. The Need for High Sampling Density in Formamide Conformational Analysis.* Journal of Computational Chemistry, 1990. **11**(3): p. 361-373.

Appendix A: Adsorption, Diffusion and Membrane Selectivities and S_{sp} Values of ZIFs

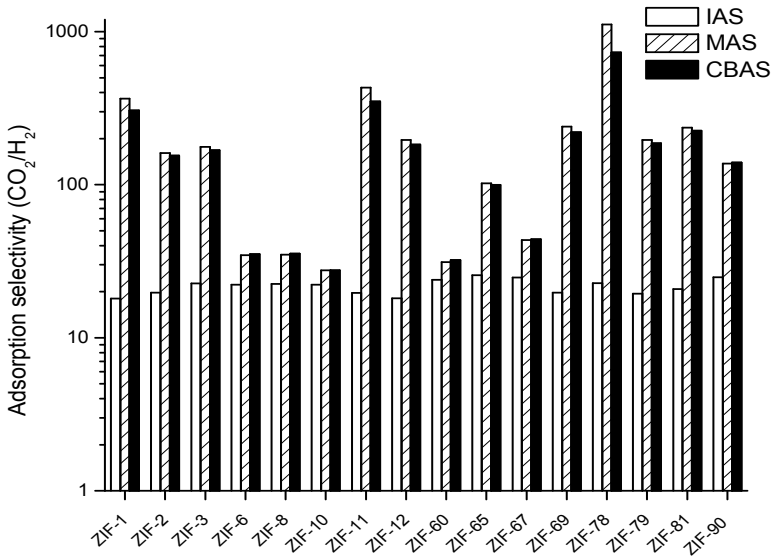

Figure A1. Adsorption selectivity of ZIFs for CO_2 in CO_2/H_2 at 298 K and 10 bar. The composition of CO_2/H_2 is 1/99.

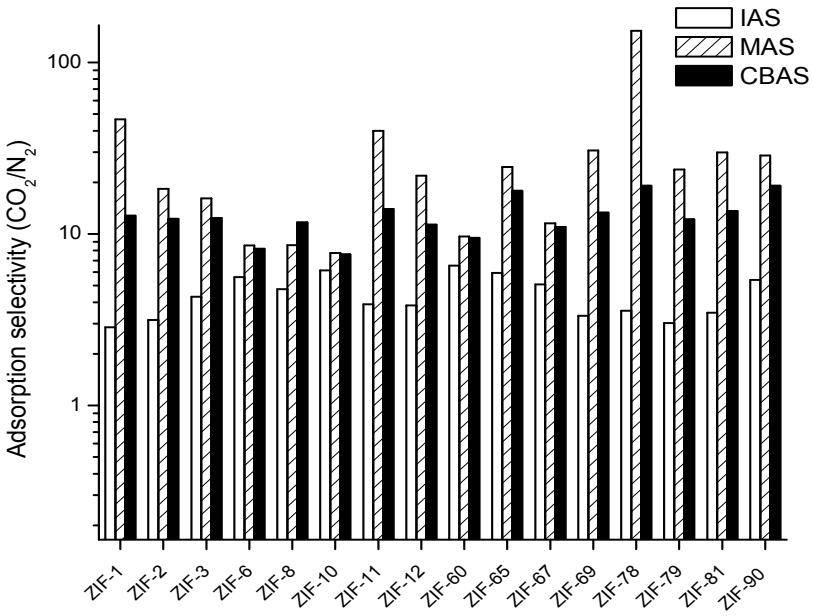

Figure A2. Adsorption selectivity of ZIFs for CO_2 in CO_2/N_2 at 298 K and 10 bar. The composition of CO_2/N_2 is 15/85.

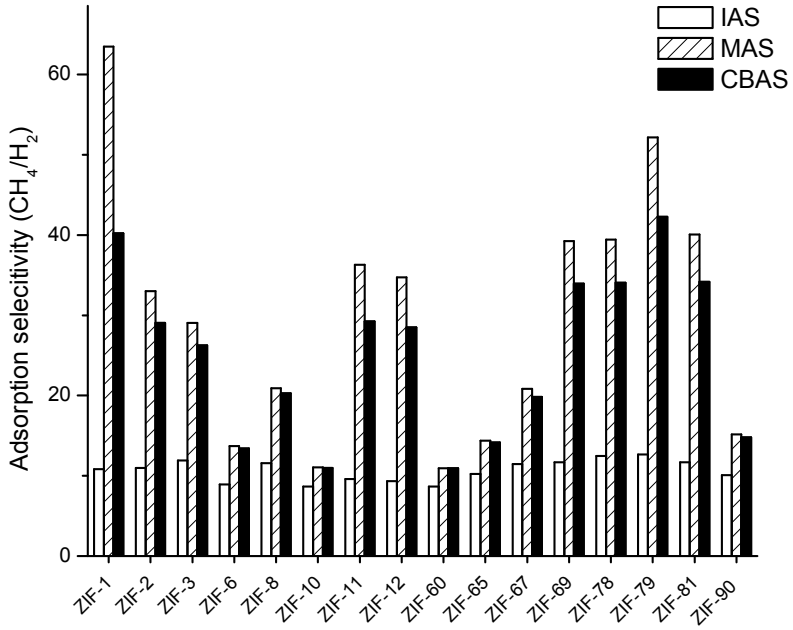

Figure A3. Adsorption selectivity of ZIFs for CH_4 in CH_4/H_2 at 298 K and 10 bar. The composition of CH_4/H_2 is 10/90.

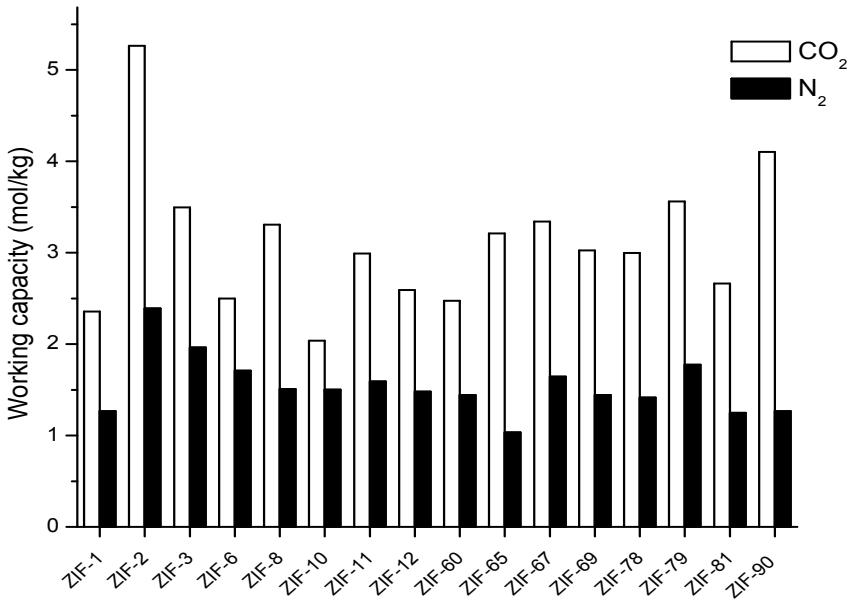

Figure A4. Working capacity of ZIFs for CO_2 and N_2 in CO_2/N_2 (15/85) at 298 K. Adsorption and desorption pressures are 10 and 1 bar, respectively.

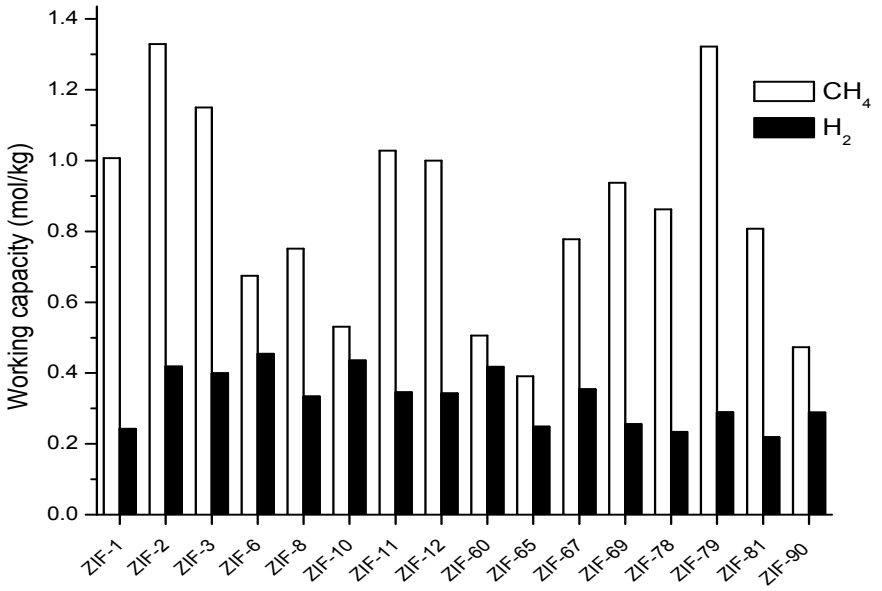

Figure A5. Working capacity of ZIFs for CH_4 and H_2 in CH_4/H_2 (10/90) at 298 K. Adsorption and desorption pressures are 10 and 1 bar, respectively.

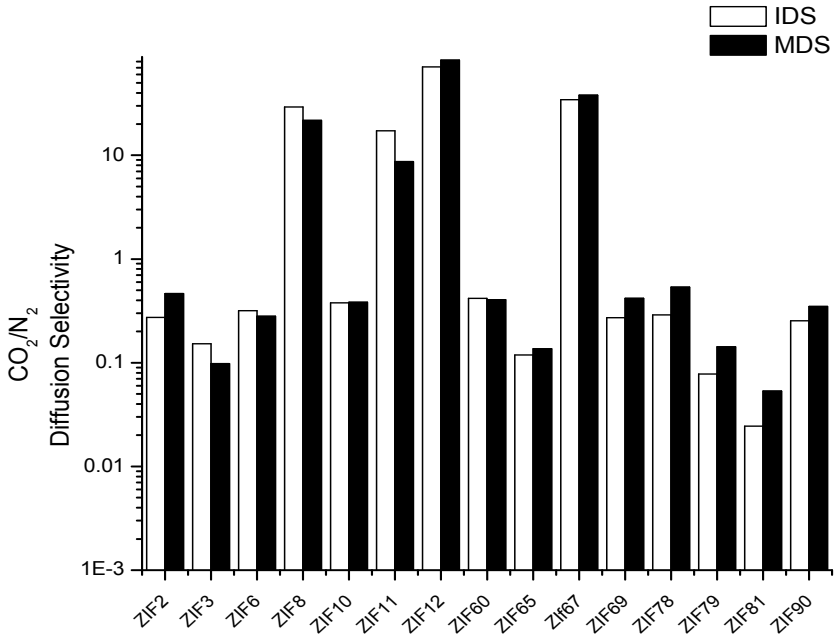

Figure A6. Diffusion selectivities of ZIFs for CO_2 in CO_2/N_2 at 298 K and 10 bar. The composition of CO_2/N_2 is 15/85.

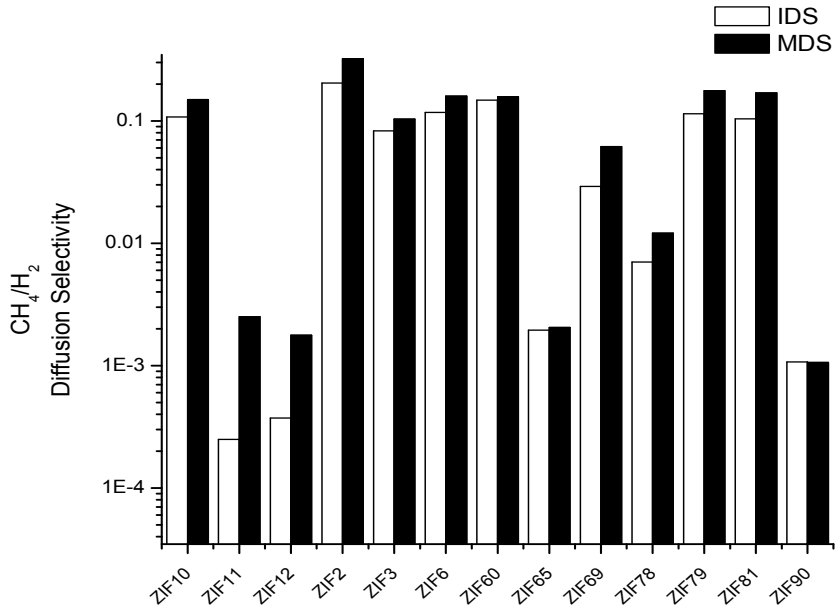

Figure A7. Diffusion selectivities of ZIFs for CH_4 in CH_4/H_2 at 298 K and 10 bar. The composition of CH_4/H_2 is 10/90.

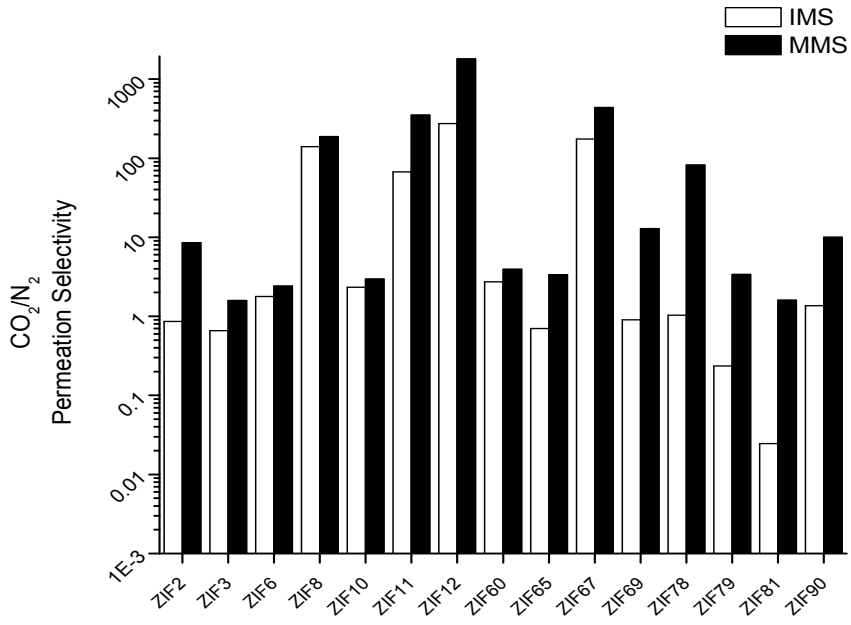

Figure A8. Permeation selectivities of ZIFs for CO_2 in CO_2/N_2 at 298 K and 10 bar. The composition of CO_2/N_2 is 15/85.

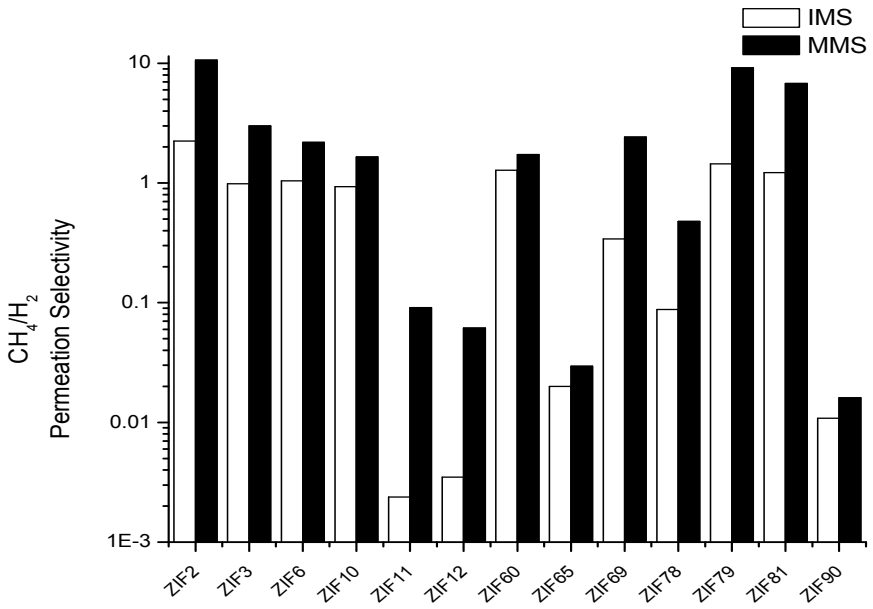

Figure A9. Permeation selectivities of ZIFs for CH_4 in CH_4/H_2 at 298 K and 10 bar. The composition of CH_4/H_2 is 10/90.

Appendix B: Atomic Representation and Validation Figures of ZIF-68 and ZIF-69

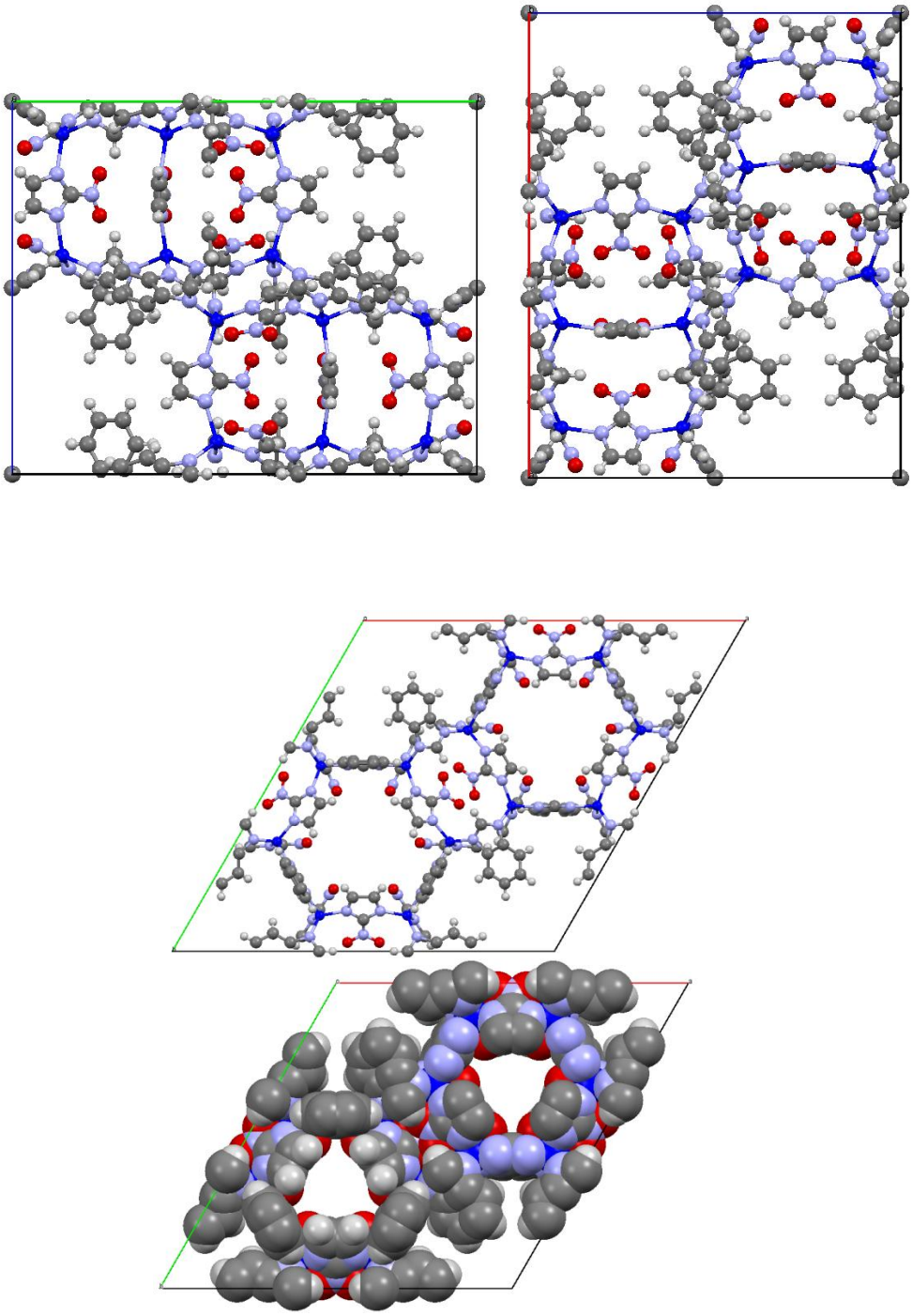

Figure B1. Atomic representations of ZIF-68 in a (upper left), b (upper right), c (lower left) directions. Pores of ZIF-68 in c direction (lower right). Grey: C, purple: N, red: O, white: H, blue: Zn.

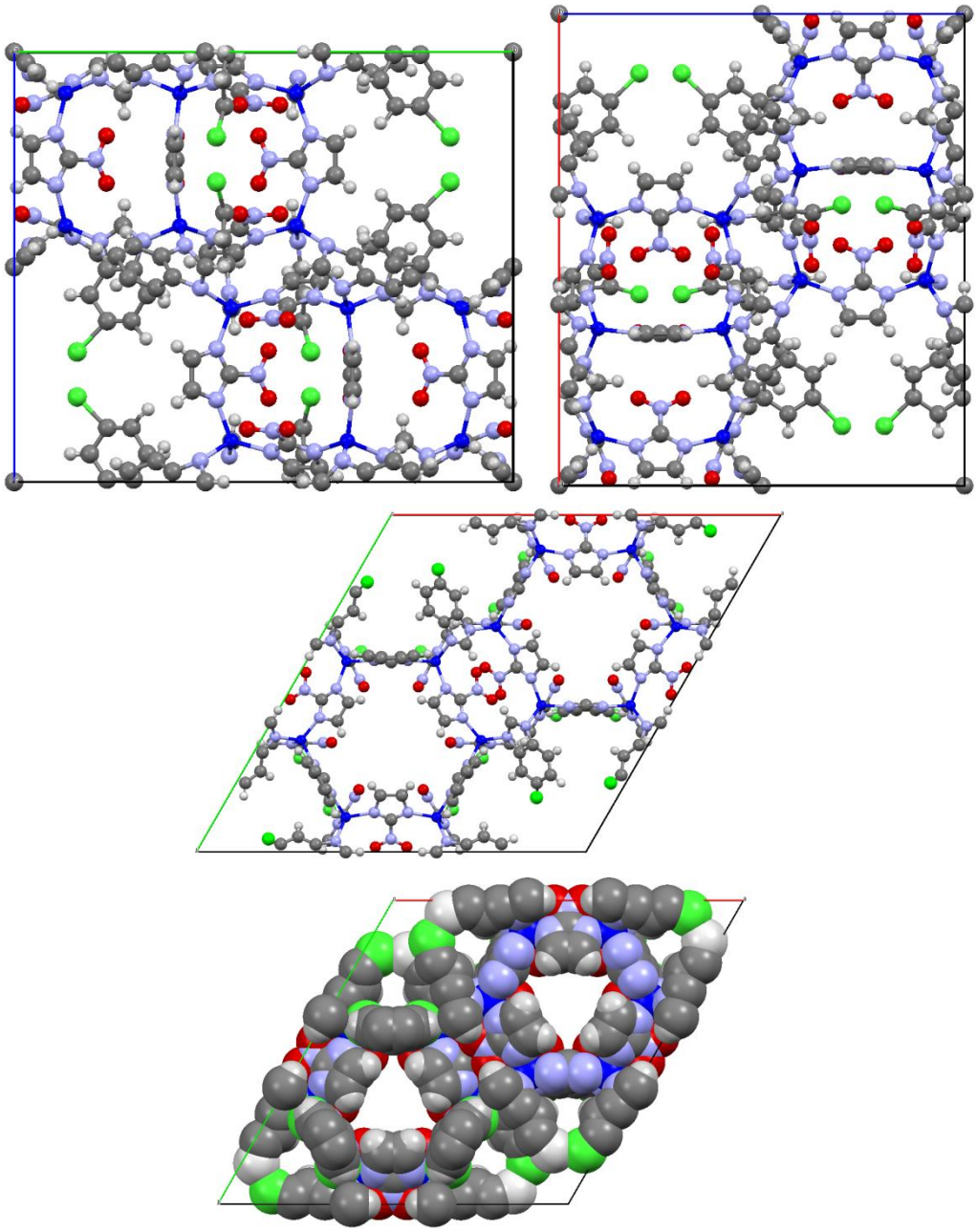

Figure B2. Atomic representations of ZIF-69 in a (upper left), b (upper right), c (lower left) directions. Pores of ZIF-69 in c direction (lower right). Grey: C, purple: N, green: Cl, red: O, white: H, blue: Zn.

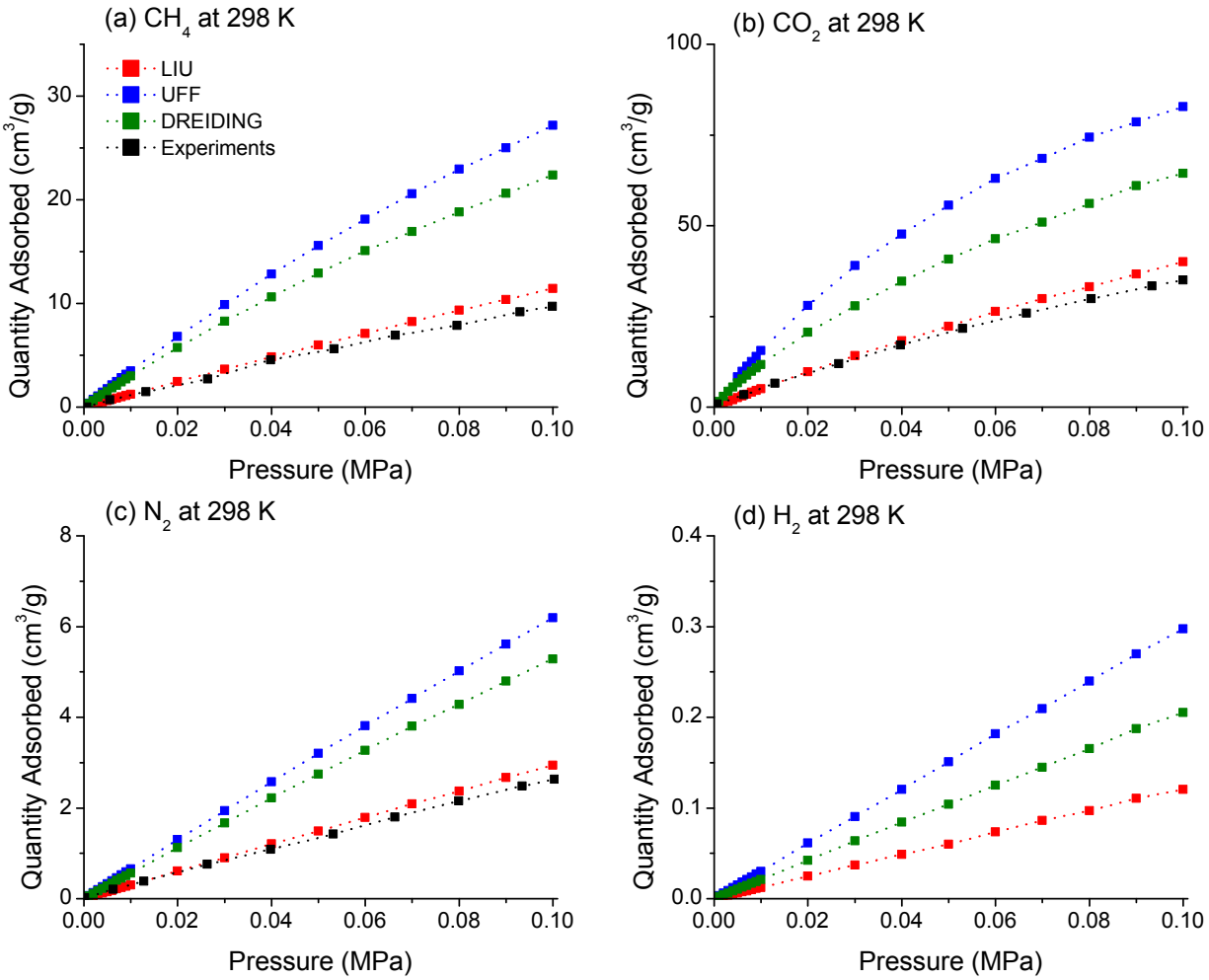

Figure B3. Comparison of experiments [34] and molecular simulation results for single-component adsorption isotherms of (a)CH_4, (b)CO_2, (c)N_2 and (d)H_2 at 298 K in ZIF-68.

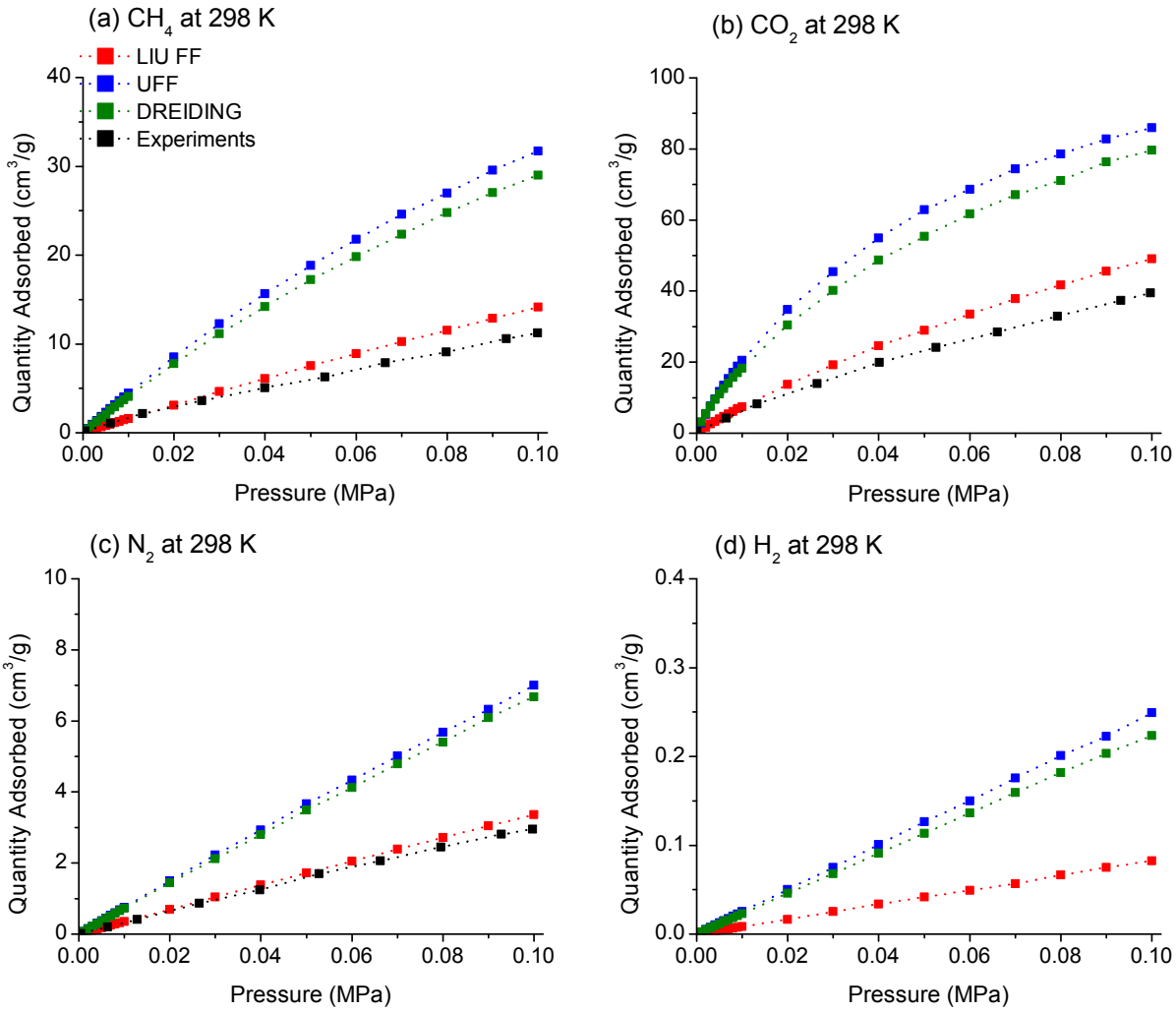

Figure B4. Comparison of experiments [34] and molecular simulation results for single-component adsorption isotherms of (a)CH_4, (b)CO_2, (c)N_2 and (d)H_2 at 298 K in ZIF-69.

Table B1. Force field parameters and partial atomic charges used in molecular simulations of ZIF-68 and ZIF-69 together with potential parameters of gas molecules.

Gases/ZIFs	Parameters/Charges	Zhong [40]	Liu [39]	Babarao [47]	Atci [53]	In Chapter 6
CO_2	ε_C/k_B (K)	52.84	29.66	29.66	27.00	29.66
	ε_O/k_B (K)	30.19	82.96	82.96	79.00	82.96
	σ_C (Å)	3.43	2.78	2.78	2.80	2.78
	σ_O (Å)	3.12	3.01	3.01	3.05	3.01
	q_C (e)	0.54	0.57	0.57	0.70	0.57
	q_O (e)	-0.27	-0.28	-0.28	-0.35	-0.28
N_2	ε_N/k_B (K)		36.00	36.40	36.40	36.00
	σ_N (Å)		3.31	3.32	3.31	3.31
	q_N (e)		-0.48	-0.48	-0.40	-0.48
	q_{COM} (e) (COM:center of mass)		0.96	0.96	0.80	0.96
CH_4	ε_{CH4}/k_B (K)		158.50	158.50	148.00	158.50
	σ_{CH4} (Å)		3.72	3.72	3.73	3.72
H_2	ε_{H2}/k_B (K)			12.50	34.20	34.20
	σ_{H2} (Å)			2.59	2.96	2.96
ZIF-68	Parameters of atoms	UFF	Liu FF	UFF DREIDING		UFF DREIDING Liu FF
ZIF-69	Parameters of atoms	UFF	Liu FF	UFF DREIDING	UFF DREIDING	UFF DREIDING Liu FF
ZIF-68	Partial charges	Accelrys Dmol^3 [105]	Zhong et al. [40]	Rankin et al. [52]	CBAC [78]	Zhong et al. [40]
ZIF-69	Partial charges	Accelrys Dmol^3 [105]	Adopted from Zhong et al. [40]	ChelpG [106]	CBAC [78]	Liu et al. [39]

Table B2. Effects of FFs on the predicted gas separation performance of ZIF-68. The composition of CH_4/H_2, CO_2/CH_4, CO_2/H_2, CO_2/N_2 and CH_4/N_2 mixtures are set to 50/50, 50/50, 1/99, 15/85 and 50/50, respectively. Adsorption (feed) and desorption (permeate) pressures of adsorbents (membranes) are set to 1 MPa (1 MPa) and 0.1 MPa (vacuum) at 298 K.

ZIF-68	**FF**	**CH_4/H_2**	**CO_2/CH_4**	**CO_2/H_2**	**CO_2/N_2**	**CH_4/N_2**
Adsorption selectivity	UFF	31.93	5.62	202.94	27.25	4.82
	DREIDING	28.51	5.01	173.03	22.33	4.51
	Liu FF	18.39	5.10	77.86	15.69	3.74
Diffusion selectivity	UFF	0.14	0.10	0.0087	0.09	0.74
	DREIDING	0.20	0.12	0.0092	0.09	0.71
	Liu FF	0.11	0.14	0.0140	0.13	0.75
Permeation selectivity	UFF	4.72	0.57	1.78	2.61	3.60
	DREIDING	5.75	0.65	1.59	2.06	3.21
	Liu FF	2.13	0.72	1.09	2.11	2.81
Working capacity of the 1st component (mol gas/kg ZIF)	UFF	2.43	3.53	0.58	2.99	2.17
	DREIDING	2.07	3.26	0.43	2.43	1.86
	Liu FF	1.63	3.27	0.19	1.82	1.51
S_{sp}	UFF	719.26	41.74	407.18	149.16	21.70
	DREIDING	509.48	30.29	239.72	91.01	18.14
	Liu FF	309.39	32.32	59.72	45.63	14.30
Regenerability (%)	UFF	77.67	60.45	88.54	75.88	76.32
	DREIDING	78.23	65.22	86.33	77.56	76.70
	Liu FF	85.52	70.24	89.22	84.52	84.71
Permeability of the 1st component (Barrer/10^4)	UFF	7.69	1.36	7.64	3.00	5.58
	DREIDING	6.20	1.06	4.92	2.17	4.10
	Liu FF	5.79	1.82	4.76	2.95	4.89

Table B3. Effects of FFs on the predicted gas separation performance of ZIF-69. The composition of CH_4/H_2, CO_2/CH_4, CO_2/H_2, CO_2/N_2 and CH_4/N_2 mixtures are set to 50/50, 50/50, 1/99, 15/85 and 50/50, respectively. Adsorption (feed) and desorption (permeate) pressures of adsorbents (membranes) are set to 1 MPa (1 MPa) and 0.1 MPa (vacuum) at 298 K.

ZIF-69	FF	CH_4/H_2	CO_2/CH_4	CO_2/H_2	CO_2/N_2	CH_4/N_2
Adsorption selectivity	UFF	42.72	5.99	311.68	35.87	5.52
	DREIDING	40.60	6.06	288.86	22.33	6.05
	Liu FF	25.34	5.10	132.37	20.06	4.19
Diffusion selectivity	UFF	0.11	0.27	0.005	0.14	0.49
	DREIDING	0.13	0.29	0.009	0.17	0.50
	Liu FF	0.09	0.29	0.011	0.18	0.70
Permeation selectivity	UFF	5.05	1.64	1.79	5.06	2.73
	DREIDING	5.29	1.77	2.83	3.82	3.07
	Liu FF	2.36	1.51	1.56	3.74	2.95
Working capacity of the 1st component (mol gas/kg ZIF)	UFF	2.45	2.60	0.75	2.82	2.21
	DREIDING	2.16	2.70	0.65	2.19	2.38
	Liu FF	1.81	2.94	0.28	1.98	1.64
S_{sp}	UFF	1249.29	43.90	811.60	276.95	28.73
	DREIDING	1161.43	49.40	512.68	91.01	34.49
	Liu FF	806.85	32.32	162.74	73.32	18.15
Regenerability (%)	UFF	74.40	50.05	85.92	69.96	72.71
	DREIDING	75.55	54.03	81.99	77.56	74.05
	Liu FF	83.86	70.24	88.28	80.93	82.88
Permeability of the 1st component (Barrer/10^4)	UFF	3.25	0.48	3.61	1.11	1.21
	DREIDING	3.67	0.68	5.53	1.17	1.28
	Liu FF	2.32	0.75	2.93	1.50	1.39

VITA

Aydın Özcan was born in Amasya, Turkey. In 2007, he graduated from Material Science Department of Sabancı University with a minor degree in Physics. He successfully got his MSc degree from Chemical and Biological Engineering Department at Koç University. His research interests include physics and chemistry related material science problems. He will continue his PhD study in Department of Physics, Koç University.

Publications:

- Ozcan, A. and Keskin, S. (2014) "Effect of Molecular Simulation Parameters on Predicting Gas Separation Performance of ZIFs" Journal of Chemical Technology and Biotechnology, Accepted for publication, DOI: 10.1002/jctb.4482
- Yilmaz, G., Ozcan, A. and Keskin, S. (2014) "Computational Screening of ZIFs for CO_2 Separations" Molecular Simulation, Accepted for publication, DOI:10.1080/08927022.2014.923568